

StockFormer: A Swing Trading Strategy Based on STL Decomposition and Self-Attention Networks

Abstract

Amidst ongoing market recalibration and increasing investor optimism, the U.S. stock market is experiencing a resurgence, prompting the need for sophisticated tools to protect and grow portfolios. Addressing this, we introduce "Stockformer," a cutting-edge deep learning framework optimized for swing trading, featuring the TopKDropout method for enhanced stock selection. By integrating STL decomposition and self-attention networks, Stockformer utilizes the S&P 500's complex data to refine stock return predictions. Our methodology entailed segmenting data for training and validation (January 2021 to January 2023) and testing (February to June 2023). During testing, Stockformer's predictions outperformed ten industry models, achieving superior precision in key predictive accuracy indicators (MAE, RMSE, MAPE), with a remarkable accuracy rate of 62.39% in detecting market trends. In our backtests, Stockformer's swing trading strategy yielded a cumulative return of 13.19% and an annualized return of 30.80%, significantly surpassing current state-of-the-art models. Stockformer has emerged as a beacon of innovation in these volatile times, offering investors a potent tool for market forecasting. To advance the field and foster community collaboration, we have open-sourced Stockformer, available at [Stockformer GitHub repository](#).

Keywords: US Stock Market, Transformer, S&P 500, Return Rate Forecasting, Layered Backtesting

1. Introduction

1.1. Background

1.1.1. Deep Learning in Stock Investment

Deep learning algorithms, akin to the neural networks of the human brain, capitalize on large datasets to train models capable of sophisticated analysis [Zhou, Zhang & Linna \(2023\)](#). These models excel in feature extraction and prediction in various domains, such as computer vision and recognition tasks [Li, Hu & Luo \(2023\)](#).

In quantitative investment, deep learning offers novel avenues for enhancing multi-factor strategies, which are fundamental in discerning stock price movements [Wang, Zhuang & Feng \(2022\)](#). By automating feature learning and capturing non-linear relationships, deep learning algorithms can effectively identify complex patterns in stock market data [Wang & Huang \(2022\)](#).

Globally, researchers have recognized the potential of deep learning in forecasting market trends. Preliminary studies using deep neural networks to predict stock and futures prices have shown encouraging results [Zhou et al. \(2023\)](#). While the domestic application of deep learning has been concentrated in securities firms and funds primarily through recurrent neural networks (RNNs), convolutional neural networks (CNNs) have also shown potential in processing stock information as two-dimensional data, thus broadening the scope of quantitative investment strategies [Li et al. \(2023\)](#).

1.1.2. Rising Popularity of Alpha Strategy

The Alpha strategy aims to differentiate returns by focusing on the Alpha component, which is unaffected by systematic risks [Guo, Wang, Ni & Shum \(2022\)](#). This strategy is gaining traction as it enables market-neutral portfolios to generate consistent profits irrespective of market direction, by hedging Beta risk with financial derivatives [Yue, Liu & Zhang \(2022\)](#).

Incorporating the Alpha strategy into Swing Trading can accentuate a trader's ability to leverage short-term price movements, focusing on stock-specific returns [Aboussalah, Xu & Lee \(2021\)](#). Compared to traditional investment vehicles, the Alpha strategy's higher returns and lower risks make it an attractive choice for swing traders aiming for market outperformance on a risk-adjusted basis.

The current market conditions and investor preferences lean towards absolute return strategies that target Alpha returns. While traditional econometric models have been utilized to gauge hedging ratios, the integration of deep learning algorithms, such as autoencoders, could potentially revolutionize the Alpha Strategy within Swing Trading by uncovering complex trend correlations [Huang, Cai, Feng & Xie \(2023\)](#), thereby enhancing the pursuit of higher Alpha returns [Yue et al. \(2022\)](#).

1.2. Research Objectives and Importance

Traditional stock prediction methods typically hinge on historical price data, with underlying assumptions such as normal distribution, stationarity, and linearity. However, these methods

struggle to encapsulate the full complexity of stock data, which is rich in time series information and influenced by an array of factors including political, economic, and cultural elements.

Neural networks represent a paradigm shift in this realm. As nonlinear, large-scale, and adaptive systems with numerous interconnected processing units, they excel in their ability to approximate nonlinear functions, adapt to new patterns, tolerate faults, and process information in parallel. In the domain of stock forecasting, neural networks have the capacity to identify subtle patterns and regularities within historical data to anticipate future trends, outperforming traditional models by adapting to the market's multifaceted nature. Therefore, leveraging neural networks for predicting stock trends promises enhanced precision and reliability.

1.3. Research Innovations

Our research introduces novel contributions to stock return prediction utilizing deep learning techniques:

1. We enhance factor construction by building on the industry's volume-price factors and applying feature engineering to expand our factor library. This allows for a more comprehensive capture of elements influencing stock returns.
2. For model architecture, we develop a multifaceted Stockformer framework that integrates various predictors for a holistic analysis.

On the Temporal Dimension.

1. STL decomposition is utilized innovatively to disaggregate stock returns into trend and seasonal components. This separation facilitates the discernment of both long-term growth trends and short-term cyclical patterns. We introduce a dual-channel spatiotemporal encoder to capture these dual-scale temporal dynamics. Fusion attention mechanisms aggregate these patterns, and multiple predictive supervisions are employed to forecast the sequence of future trends, which operate concurrently with the main return prediction task.
2. Beyond utilizing return features alone, we incorporate 158 multifactorial inputs to construct a comprehensive model. This approach extends our analysis to a multivariate time series framework, enhancing the prediction's accuracy and resilience to market variations.

On the Spatial Dimension.

1. To capture the correlation between stocks and their returns, our approach constructs a stock space graph. This graph quantifies the relationships by calculating Spearman correlation coefficients between stock returns, establishing stocks as nodes and these coefficients as the edges' weights. To deeply understand the network's structure, we apply struc2vec to learn the nodes' embedding representations, which reflect their structural roles and mutual interactions, providing a high-dimensional perspective of the stock space.
2. Acknowledging the periodic behavior of stock returns, we propose the construction of a temporal graph. This graph transforms the concept of time into a connected structure, embedding temporal patterns such as monthly and weekly cycles into the network. Each time slot is modeled as a node, with edges representing the temporal linkages. Through graph embedding techniques, we obtain representative vectors for these nodes, capturing the essential temporal features of the stocks.

2. Literature Review

2.1. Factor Construction

A factor is a quantifiable variable that influences stock returns, encapsulating the underlying economic and financial dynamics. The conventional factors encompass market, style, industry, macroeconomic, price-volume, and machine learning-derived factors. The seminal works of [Fama & French \(1992\)](#) and [Fama & French \(2015\)](#) introduced market factors such as excess returns and volatility, encapsulating the overall market performance and risk. [Green, Hand & Zhang \(2017\)](#) utilized cross-sectional regression on 94 US stocks to investigate style factors, shedding light on the relative performance of diverse stock categories.

Our study primarily leverages price-volume factors and augments them with machine learning-derived factors through feature engineering. This approach is designed to refine the input for deep learning models, enhancing their predictive capability.

2.2. Time Series Decomposition Method

Assuming that a time series is obtained by adding multiple components, it can be expressed in the following form:

$$y_t = S_t + T_t + R_t \tag{1}$$

Where, y_t represents the time series data, S_t represents the seasonal component, T_t represents the trend-cycle component, and R_t represents the residual component. Additionally, the time series can also be expressed in a multiplicative form:

$$y_t = S_t \times T_t \times R_t \quad (2)$$

The additive model, chosen when seasonal fluctuations and trend-cycle variations do not scale with the time series, is celebrated for its strong explanatory power and its prowess in isolating irregular components, making it particularly useful in economic time series analysis [Huang, Shen, Long, Wu, Shih, Zheng, Yen, Tung & Liu \(1998\)](#); [Chen & Wang \(2012\)](#); [Bonizzi, Karel, Meste & Peeters \(2014\)](#). In contrast, the multiplicative model is favored when these changes are proportional to the time series level. The classical decomposition method, utilizing moving averages for component estimation, has been a mainstay for its simplicity and efficacy in datasets with stable seasonal patterns [Singh \(2018\)](#).

As the need for sophisticated seasonal adjustments grew, so did the refinement of decomposition techniques. The X11 method, an advanced form of the classical method, offers a more comprehensive seasonal adjustment by considering additional factors like calendar effects [Dagum & Bianconcini \(2016\)](#). The SEATS method leverages ARIMA modeling to fit trend and seasonal components, plus frequency domain analysis for non-periodic components, making it apt for a wide range of macroeconomic and financial time series [Dagum & Bianconcini \(2016\)](#). The STL method, grounded in locally weighted regression, excels in handling non-linear and non-stationary time series, and its application extends across diverse sectors such as meteorology and economics [Huang et al. \(1998\)](#).

In this study, we apply the STL decomposition to unravel stock return series into trend, seasonal, and residual components. These decomposed elements are then adeptly utilized as inputs to our network model, with the aim of capturing and analyzing the intricate dynamics at play within the financial markets.

2.3. Model Prediction

Model selection in securities trading data, given its variety and temporal characteristics, encompasses both static and dynamic approaches.

Historically, before the proliferation of deep learning, time series models such as ARIMA and GARCH were the go-to methods across multiple domains, including finance [Qian & Gao \(2017\)](#). The machine learning era introduced novel techniques capable of managing high-dimensional and sequential data complexities. For instance, representation learning has been applied in clinical time series data within electronic health records to enhance prediction tasks [Ruan, Lei, Zhou, Zhai, Zhang, He & Gao \(2019\)](#), and models like the backpropagation bidirectional extreme learning machine (BP-BELM) have found use in traffic flow predictions [Zou & Xia \(2018\)](#).

Deep learning extends the focus to the temporal and spatial attributes of data, advancing beyond mere time series to spatiotemporal predictions, with applicability across diverse fields. Yuan et al. [Yuan, Li, Bao & Feng \(2020\)](#) depicted temporal periodicity through undirected graphs in traffic series prediction, while Ribeiro et al. [Ribeiro, Saverese & Figueiredo \(2017\)](#) leveraged structural homophily to learn node representations, enhancing graph embedding with the struc2vec method. Fang et al. [Fang, Qin, Luo, Zhao, Xu, Wang & Zeng \(2021\)](#) utilized discrete wavelet transforms on traffic data, segregating it into frequency components and employing graph convolution and spectral attention mechanisms. Providence et al. [Providence, Yang, Orphe, Mabaire & Agordzo \(2022\)](#) improved prediction accuracy in multivariate series by normalizing them spatially with the ST norm and testing a Wavenet-Transformer combination on public datasets.

This study integrates deep learning techniques for stock prediction. We employ STL decomposition on stock factors and labels to achieve decoupling. Subsequently, we utilize a dual-channel approach, encoding seasonal and trend components through time attention networks and dilated causal convolution networks. By incorporating time graph embedding and spatial graph embedding, we enhance the model with spectral graph attention, and ultimately, we apply a fusion attention method for decoding to construct the factor-return relationship model.

2.4. Backtesting Trading Strategy

[Fung & Hsieh \(1997\)](#) delves into the empirical characteristics of dynamic trading strategies utilized by hedge funds. The study introduces a methodology for backtesting and evaluating investment strategies, offering invaluable insights into the performance evaluation and risk management of dynamic trading strategies. [Georgakopoulos \(2015\)](#) presents the application of the R programming language for backtesting investment strategies. The research outlines the crucial stages in data procurement, strategy execution, performance assessment, and risk management. It

serves as a practical guide, providing examples for those keen on employing R for backtesting trading strategies. [Chan \(2021\)](#) elucidates the foundational principles of quantitative trading and the intricacies of strategy formulation. The study touches upon essential facets of backtesting methods, data manipulation, strategy assessment, and risk management. It furnishes practical techniques and case studies, aiding readers in comprehending and implementing backtesting trading strategies. [De Prado \(2018\)](#) investigates the integration of machine learning in finance, encompassing backtesting methods and techniques. A novel backtesting approach termed "out-of-sample" testing is introduced, aiming to bolster strategy resilience by circumventing over-reliance on historical data. [Qian, Hua & Sorensen \(2007\)](#) centers on quantitative equity portfolio management methodologies and techniques. The research encompasses pivotal elements of backtesting and optimization of investment strategies, spanning data collection, strategy execution, performance assessment, and risk management. Collectively, these studies furnish theoretical insights, hands-on guidance, and case studies pertinent to backtesting trading strategies. Nonetheless, numerous facets remain uncharted, signaling opportunities for continued exploration and advancement in this domain.

2.5. Backtesting Trading Strategy

Backtesting trading strategies is an integral part of the investment process, enabling the assessment of strategy performance and risk management before real-world application. Fung and Hsieh [Fung & Hsieh \(1997\)](#) provide an empirical examination of hedge funds' dynamic trading strategies, establishing a framework for backtesting and evaluation. Georgakopoulos [Georgakopoulos \(2015\)](#) demonstrates the utility of R for backtesting, detailing processes from data acquisition to strategy implementation and risk assessment. Chan [Chan \(2021\)](#) offers a thorough overview of quantitative trading foundations, with a focus on backtesting, data handling, and strategy execution. De Prado's work [De Prado \(2018\)](#) highlights the convergence of machine learning with financial backtesting, introducing "out-of-sample" testing to enhance strategy robustness. Qian [Qian et al. \(2007\)](#) discusses quantitative equity portfolio management, covering backtesting and optimization across strategy development and performance evaluation. Together, these contributions provide theoretical frameworks, practical insights, and extensive case studies for backtesting trading strategies. Despite these advancements, there is still unexplored territory in backtesting, suggesting room for further research and innovation in strategy development and validation.

3. Methodology

3.1. STL Decomposition of Stock Return Sequence

3.1.1. STL Decomposition Theoretical Basis

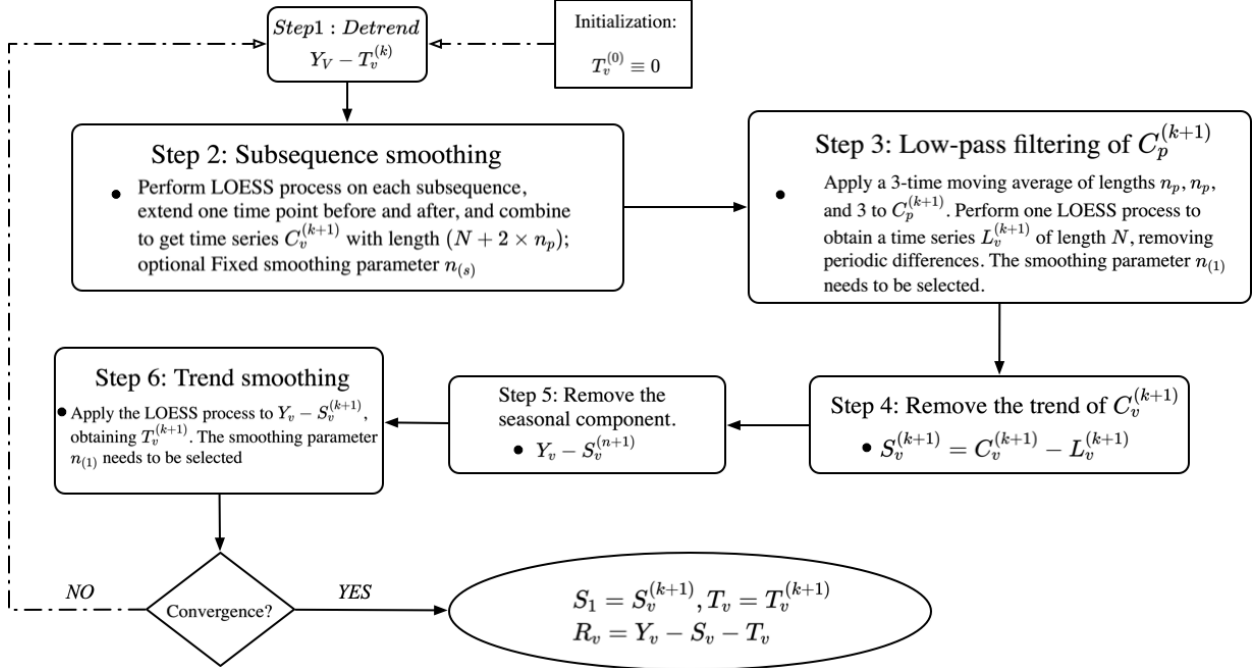


Figure 1: STL decomposition inner loop algorithm

Seasonal and Trend Decomposition using Loess, STL, is a flexible and resilient technique widely used for time series decomposition. It stands for "Seasonal and Trend decomposition using Loess," where Loess refers to a method for estimating nonlinear relationships. The development of the STL method can be attributed to [Cleveland, Cleveland, McRae & Terpenning \(1990\)](#).

STL has several advantages in time series analysis. Firstly, it effectively separates the components of a time series, namely trend, seasonal pattern, and residuals. This decomposition enables a better understanding of the underlying structure and patterns in the data. Moreover, STL employs the Loess method, which is particularly useful for capturing and estimating nonlinearity in time series.

The STL decomposition process involves two iterative steps: an internal cycle and an external cycle. The internal cycle is responsible for fitting the trend and determining the seasonal component. The inner loop is shown in [Figure 1](#).

3.1.2. Measuring strength of trend and seasonality

The degree of trend and seasonal components in a time series can be determined using the method proposed by Wang, Smith & Hyndman (2006). Two indicators, F_T and F_S , are defined to measure the relative strength of the trend and seasonal components, respectively, in a time series data. F_T is calculated as the variance of the residual component R_t divided by the variance of $T_t + R_t$, where T_t is the trend component. Similarly, F_S is calculated as the variance of R_t divided by the variance of $S_t + R_t$, where S_t is the seasonal component.

$$F_T = \max\left(0, 1 - \frac{\text{Var}(R_t)}{\text{Var}(T_t + R_t)}\right) \quad (3)$$

$$F_S = \max\left(0, 1 - \frac{\text{Var}(R_t)}{\text{Var}(S_t + R_t)}\right) \quad (4)$$

These indicators help in assessing the relative importance of trend and seasonal components in the time series data. High F_T and F_S values indicate that the trend and seasonal components, respectively, contribute significantly to the variations in the time series data. These measurements are useful for identifying time series with strong trend or seasonal characteristics for further analysis and application.

3.2. Self-Attention Mechanism

The self-attention mechanism is a prevalent approach that empowers each element in a sequence to aggregate information from all other tokens in the sequence. The mechanism processes inputs composed of queries, keys, and values, each having a dimension d . The procedure involves computing the dot products of the query with all the keys, dividing each by \sqrt{d} , and then applying a softmax function to obtain the weights on the values. Mathematically, this operation can be represented as:

$$\text{Att}(Q, K, V) = \text{softmax}\left(\frac{(QW^Q)(K^TW^K)}{\sqrt{d}}\right)(VW^V), \quad (5)$$

where W^Q , W^K , and W^V are the learnable parameters of the projections, and $\text{Att}(\cdot)$ denotes the self-attention operation.

3.3. Stock Return Forecasting Model

To reasonably predict stock returns, we establish a model based on multi-factors STL decomposition and self-attention network, named StockFormer. The detailed network architecture of the designed StockFormer model is shown in Figure 2. The model consists of a decoupling flow layer, a Bi-component spatiotemporal encoder, and a Component-specific decoder. The decoupling flow layer adopts STL time series decomposition to decompose stock returns into trend, seasonal, and residual components, avoiding interference between them. The trend component is used to fit the trend of stock returns, while the seasonal component is used to capture the seasonal effects of the stock market. The Bi-component spatiotemporal encoder is composed of L layers stacked together, aiming to effectively represent the bi-component spatiotemporal patterns of the trend and seasonal components. Subsequently, in the Component-specific decoder, the fused attention network is used to merge and utilize the bi-component information.

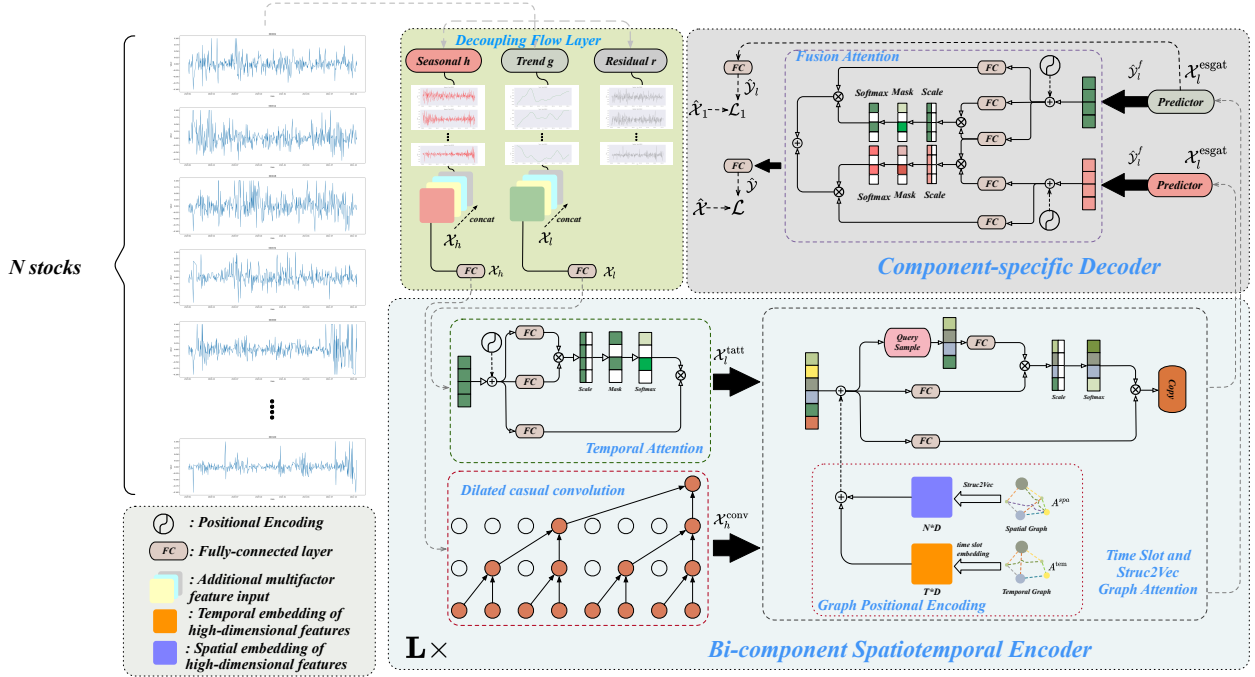


Figure 2: StockFormer Network Architecture

3.3.1. Decoupling Flow Layer

Given the return series of multiple stocks $\mathcal{X} \in \mathbb{R}^{T_1 \times N \times d}$, where T_1 represents the length of the training set, N represents the number of stocks selected from the stock pool, and d represents the

dimension of the input features including returns and multiple factors, we use STL to obtain the component series of seasonal, trend, and residual components from the entangled flow layer. The bi-component represents the seasonal and trend time patterns, because the trend component is stable and has a long-term trend, i.e., the trend of returns; the volatile seasonal component has a short-term impact, i.e., the seasonal effect in the stock market under the influence of economics, politics, environment, etc. The STL with input return series \mathcal{X}_t can be represented as in Equation 22:

$$\mathcal{X}_t = S_t + T_t + R_t \quad (6)$$

Where, y_t represents the time series data, S_t represents the seasonal component, T_t represents the trend component, and R_t represents the residual component.

To ensure the accuracy of the seasonal component period, we perform a 10-order lagged Ljung-Box test on the residual component R_t of all stock return series. If the residual series of 500 stock return series after STL decomposition all pass the Ljung-Box test and are white noise series, it is considered that the STL decomposition of the stock return series is effective, and the trend component T_t and seasonal component S_t contain most of the information of the stock returns. Through continuous testing and mining of all residual series, the final determined period is 50 days, which means there is a small cycle pattern with a period of 50 days in the stock return series. We know that there are usually about 250 trading days in a year. Through data mining, we obtained a cycle period of 50 trading days, so there are 5 cycle periods in a year. This has important economic implications and theoretical support for modeling stock return series, thereby guiding investment decisions and strategy formulation.

3.3.2. Bi-component Spatiotemporal Encoder

The Bi-component spatiotemporal encoder consists of time attention, temporal convolutional layer, time slot and Struc2Vec graph attention networks (GATs).

Extraction of Time Features through Decoupling. Unlike previous works that employed singular methods like LSTM to model the intricate temporal patterns in intertwined financial sequences, we utilize dilated causal convolutions and temporal attention to capture the time-relatedness of trend and seasonal components. Dilated causal convolution is a specialized one-dimensional convolution that slides over the input by skipping values at a specified stride, as

depicted in Figure 2. Theoretically, given a one-dimensional sequence input $x \in \mathbb{R}^T$ and a filter $f \in \mathbb{R}^J$, the dilated causal convolution operation between x and f at time step t is defined as in Equation 7:

$$x \star f(t) = \sum_{j=0}^J f(j)x(t - c \times j), \quad (7)$$

where c is the dilation factor. The dilated causal convolution for the seasonal component is represented in Equation 8:

$$\mathcal{X}_h^{\text{conv}} = \text{ReLU}(\Theta \star \mathcal{X}_h + b), \quad (8)$$

where Θ and b are learnable parameters, and $\text{ReLU}(\cdot)$ is the rectified linear unit. Additionally, we employ masked self-attention on the temporal dimension of the trend component, as the low-frequency component is stable and can represent the clear long-term trend of returns:

$$\begin{aligned} \mathcal{X}_l^{\text{tatt}} &= \text{Concat}(ta_1, \dots, ta_n, \dots, ta_N) \\ \text{where } ta_n &= \text{Att}(X_l^n, X_l^n, X_l^n). \end{aligned}$$

Temporal Slots and Struc2Vec Graph Attention Network.

Temporal Slots. As previously mentioned, stock returns exhibit periodic fluctuations. With each day represented as a timestamp t , and considering a day as a time unit in the dataset, it becomes essential to extract temporal features from t . An intuitive approach is to treat each timestamp as a floating-point number and design a multi-layer perceptron model to convert this value into a fixed-length vector. However, this method has two drawbacks: firstly, each timestamp is typically a large integer, which could overshadow other features. Secondly, there’s a monthly and daily periodicity between different timestamps, which cannot be captured solely by the timestamp. For instance, trading conditions on the same day of different months might be similar. To address this, we adopt the temporal slot method to represent timestamps.

Given a reference timestamp t_0 (ensuring $t - t_0 \geq 0$, t_0 must be smaller than any timestamp in the training and testing data) and a time unit Δt , time intervals such as $[t_0, t_0 + \Delta t)$, $[t_0 + \Delta t, t_0 + 2\Delta t)$, \dots can be derived. These intervals are termed as temporal slots, with each slot sized at Δt , which is a day in this dataset.

For simplicity, each temporal slot is represented by its corresponding index. For instance, $[t_0, t_0 + \Delta t)$ is represented as 0. Based on Definition 4, timestamp t can be mapped to a specific

temporal slot t^p , where $t \geq t_0$, and t^p is calculated as in Equation 9:

$$t^p = \left\lfloor \frac{t - t_0}{\Delta t} \right\rfloor \quad (9)$$

To represent each timestamp at a finer granularity, we record the time remainder t^r to ensure the uniqueness of t , where $0 \leq t^r < \Delta t$. It's calculated as in Equation 10:

$$t^r = t - t_0 - t^p \Delta t \quad (10)$$

In conclusion, each timestamp t can be represented as $\langle t^p, t^r \rangle$.

Constructing the Temporal Graph. Next, we explore how to capture temporal features by embedding temporal slots. Given the nature of the dataset, each temporal slot can represent a day. Considering the periodic fluctuations in stock returns and the monthly cycle being the most common cyclical fluctuation in economic cycles, it suffices to focus on all temporal slots within a month. With approximately 250 trading days in a year distributed across months, each month averages 21 trading days. Inspired by Li, Fu, Wang, Shahabi, Ye & Liu (2018), we attempt to construct a temporal graph to represent temporal slots and then apply graph embedding methods to initialize the temporal slot embeddings. However, Li et al. (2018) constructed an undirected graph for temporal slots, failing to capture the sequential relationship between them. Moreover, they overlooked the connection between adjacent dates, thus missing daily periodicity.

Addressing the issue at hand, we adopt the time-slot method to represent time stamps, drawing inspiration from Yuan et al. (2020). This representation is captured by the graph $G' = \langle V', E' \rangle$. In this context, each node $v' \in V'$ denotes a temporal slot. The edges in E' are categorized into two types: (1) edges connecting adjacent date slots, symbolizing contiguous temporal slots, thus providing smoothness; and (2) edges connecting adjacent months, denoting identical temporal slots in consecutive months, ensuring similarity. As an illustration, this study designates Δt as 1 day, partitioning each month into 21 distinct temporal slots. Taking into account the twelve months within a year, we construct a directed temporal graph with a size of $21 \times 12 = 252$. Ultimately, t^p can be mapped to a node $v' \in V'$, where the sequence number for v' is given by $t^p \% 252$, with $\%$ representing the modulus operator.

Embedding Temporal Slots in the Temporal Graph. Initially, one-hot encoding is used to represent each temporal slot $O_i^t \in \mathbb{R}^{|V'|}$, where $|V'|$ is the total number of nodes in the temporal

graph G' . Then, a fully connected neural network (with weight matrix $\mathbf{W} * t \in \mathbb{R}^{|V'| \times d_t}$) is designed to transform each one-hot encoded O_i^t into a fixed-length dense vector $D_i^t = \mathbf{W} * \mathbf{t}^\top O_i^t$. This embedding is used as the initial value for \mathbf{W}_t , resulting in a high-dimensional temporal graph embedding $\rho^{\text{tem}} \in \mathbb{R}^{T \times d}$. Leveraging the broadcasting property, ρ^{tem} is replicated N times, ultimately yielding ρ^{tem} with dimensions $\rho^{\text{tem}} \in \mathbb{R}^{T \times N \times d}$.

Self-Attention Encoding. After obtaining the high dimensional temporal graph embedding and the stock return association graph embedding, this study broadcasts and sums the two, concatenating them with the seasonal and trend components, respectively. This results in an input tensor for self-attention encoding. The final temporal slot and Struc2Vec graph attention network can be represented as in Equation 11:

$$\begin{aligned} \mathcal{X}^{\text{gat}} &= \text{Concat}(sa_1, \dots, sa_t, \dots, sa_{T_1}) \\ \text{where } sa \ a_t &= \text{Att}(\tilde{X}_t, \tilde{X}_t, \tilde{X}_t) \\ \text{and } \tilde{X} &= \mathcal{X} + \rho^{\text{spa}} + \rho^{\text{tem}} \end{aligned} \quad (11)$$

Thus, through the temporal slot and Struc2Vec graph attention network mechanism, this study obtains \mathcal{X}^{gat} , a vector containing structural information and localized graph characteristics. This attention mechanism is highly efficient and expressive when handling graph data.

3.3.3. Component-specific Decoder

To convert the representations encoded by the bi-component encoder into future representations in multi-step stock return predictions, this study employs a predictor (i.e., a fully connected layer) on the time dimension of $\mathcal{X}_l^{\text{gat}}$ and $\mathcal{X}_h^{\text{gat}} \in \mathbb{R}^{T_1 \times N \times d}$. Through the predictor, future representations of the trend and seasonal components, $\hat{\mathcal{Y}}_l^f$ and $\hat{\mathcal{Y}}_h^f \in \mathbb{R}^{T_2 \times N \times d}$, are obtained. Fusion attention and multi-supervision are then employed to merge the information from the trend and seasonal components, with knowledge acquired through supervision of the trend component.

In essence, within the component-specific Decoder, this study uses a predictor to forecast the future of the trend and seasonal components outputted by the bi-component encoder. Through fusion attention and multi-supervision, the study integrates the information from the trend and seasonal components.

During the prediction process, considering that the seasonal component typically corresponds to rapid or cyclical changes in the data, exhibiting high frequency and short-term fluctuations, and

given its high volatility and potential uncertainty, efficient fitting may be challenging. Meanwhile, low-frequency components generally correspond to long-term trends and global patterns in the data, exhibiting low frequency and smoother changes. Due to their persistence and stability in the data, low-frequency components have a more significant impact on predicting overall trends and long-term changes. Therefore, this study primarily extracts useful information through supervision of the low-frequency component.

Decoupled Temporal Feature Fusion. Since the goal is not to predict the trend and seasonal components but to forecast future stock returns based on these components and other factors, as illustrated in Figure 2 this study further introduces fusion attention to merge the representations of the trend and seasonal components, $\hat{\mathcal{Y}}_l^f$ and $\hat{\mathcal{Y}}_h^f$, into the stock return $\hat{\mathcal{Y}}^f \in \mathbb{R}^{T_2 \times N \times d}$, capturing future internal dependencies. Specifically, fusion attention treats the trend component as a query, extracting useful long-term and short-term information from the trend and seasonal components in two temporal attentions. Fusion attention can be represented as in Equation 12:

$$\begin{aligned} \hat{\mathcal{Y}}^f &= \text{Concat}(fa_1, \dots, fa_n, \dots, fa_N) \\ \text{where } fa_n &= \text{Att}\left(\hat{\mathcal{Y}}_l^{f^n}, \hat{\mathcal{Y}}_l^{f^n}, \hat{\mathcal{Y}}_l^{f^n}\right) + \text{Att}\left(\hat{\mathcal{Y}}_l^{f^n}, \hat{\mathcal{Y}}_h^{f^n}, \hat{\mathcal{Y}}_h^{f^n}\right). \end{aligned} \quad (12)$$

In Equation 12, this study concatenates the attention mechanism outputs fa_n for each stock n to obtain $\hat{\mathcal{Y}}^f$. Here, the attention mechanism calculates self-attention for the trend component and attention between the trend and seasonal components. Through this fusion attention mechanism, both the trend and seasonal component information can be utilized, better capturing future stock returns and internal dependencies.

Multi-Supervision. During the training process, this study employs a fully connected layer to transform the future representation of the stock sequence, $\hat{\mathcal{Y}}^f$, into the predicted value $\hat{\mathcal{Y}}$, supervised using the L_1 loss. By acquiring knowledge from the more stable trend component, the model can effectively enhance its ability to learn the long-term trend of the stock sequence, thereby achieving improved performance. Thus, the optimization objective of Stockformer is to minimize the loss function shown in Equation 13:

$$\mathcal{L} = \sum_{t=T_1+1}^{T_1+T_2} \sum_{n=1}^N |y_t^n - \hat{y}_t^n| + |y_{t_t}^n - \hat{y}_{t_t}^n| \quad (13)$$

In the aforementioned loss function, the study computes the L_1 distance loss between the predicted and actual values for each time step t and each node n . Here, x_t^n represents the actual return rate, while \hat{y}_t^n denotes the predicted return rate; x_t^n signifies the actual trend component, and \hat{y}_t^n indicates the predicted trend component. By minimizing this loss function, the model can be trained to better fit the future trend of the return rate, thereby enhancing the model's performance.

3.4. Model Revenue Prediction and Evaluation

3.4.1. IC Value Analysis

IC value is a statistical measure that measures the predictive ability of investment strategies for stock returns. In quantitative investment, IC value is used to evaluate the effectiveness of stock selection strategies. IC value is calculated by measuring the correlation between the expected and actual returns of each stock. The research frequency of this article is daily frequency. Therefore, for each day's stock data, the correlation coefficient between the expected and actual returns of all stocks was selected as the IC value at that time point, and then the average IC value of all stocks at all time points, that is, every day, was calculated.

In theory, the range of IC values is between -1 and 1. When the IC value is less than 0, it indicates a negative correlation between expected and actual returns, which is clearly not a good strategy; When the IC value is greater than 0, the correlation between expected return and actual return is positive, indicating that this is a more effective strategy as it brings positive returns. In summary, the IC value in each study should be greater than 0 as a criterion for evaluating good or bad.

This article uses a filtered alpha factor library to train the model and obtain its return rate. The output of the model, which is the predicted return rate, is treated as a single factor, and IC value analysis can be performed by comparing it with real data. Comparing the IC value with 0 can measure whether the model is effective.

3.4.2. Layered Backtesting Analysis Methodology

To rigorously evaluate the predictive power of a model in the realm of stock forecasting, it is imperative to look beyond the IC values. Layered backtesting emerges as a robust tool to scrutinize the monotonicity of factors. The procedure commences with the acquisition of a stock pool, followed by the ranking of stocks based on the factor value. The crux of the analysis lies in discerning a

monotonic relationship between returns under the purview of the given factor. In the context of a multifactor model, a pronounced factor value, coupled with its substantial contribution to the portfolio's return, signifies the factor's pronounced monotonicity within the strategy. Post-layering, one can observe five trajectories exhibiting analogous trends.

The significance of monotonicity cannot be understated in stock selection paradigms. Factors exhibiting strong monotonicity can be elevated to the status of core factors, thereby enhancing the efficacy and stability of the strategy.

3.5. Strategy Evaluation Indicators

3.5.1. Income Metrics

The primary objective of investment endeavors is to accrue returns. Consequently, return-centric metrics emerge as the pivotal indicators for assessing the efficacy of portfolio strategies.

1. **Cumulative Rate of Return:** The Cumulative Rate of Return serves as a comprehensive metric encapsulating the total return accrued over the backtesting duration. It quantifies the percentage deviation between the initial and concluding values of the period, offering a holistic insight into the strategy's performance trajectory. The mathematical representation is articulated as:

$$R_c = \prod_{t=1}^{R_t} (1 + R_t) - 1 \quad (14)$$

2. **Annualized Rate of Return:** The Annualized Rate of Return delineates the mean annualized return over the backtesting interval. This metric is instrumental for investors aiming to fathom the long-term viability of a portfolio, especially since it incorporates the time value dimension. The corresponding formula is:

$$R_y = (1 + R)^{365/(T_2 - T_1)} \quad (15)$$

3.5.2. Risk Metrics

1. **Sharpe Ratio:** The Sharpe Ratio is the excess return from taking one unit of total risk and allows for a combination of return and risk to be considered simultaneously. It means that the Sharpe ratio can not only maximize the expected return for a given level of risk, but also minimize the risk for a given level of expected return. The formula is as follows:

$$S_p = \frac{r_p - r_f}{\sigma_p} \quad (16)$$

Where r_p is the portfolio’s rate of return, r_f is the market risk-free rate of return, and σ_p is the strategy return volatility, i.e., the standard deviation of the portfolio.

2. **Maximum Retracement:** Maximum retracement is the maximum loss of a portfolio or asset over a specific time period, relative to the highest point in the portfolio’s or asset’s net worth during that time period. It reflects the limit of an investor’s tolerance for loss and is therefore often used as a measure of a portfolio’s or asset’s exposure to market volatility. Moreover, the maximum retracement determines the leverage ratio of the investment product. It magnifies the principal and allows for higher returns. The formula is as follows:

$$\text{maxdrawdown} = \frac{P - Q}{P} \quad (17)$$

Where P represents the highest net average value during the time period, and Q represents the lowest net average value after that high point.

3. **Information Ratio:** This ratio measures the excess return on a portfolio or asset per unit of active risk. Unlike the Sharpe ratio, which uses the risk-free rate of return as a reference, the information ratio uses the benchmark rate of return. A higher information ratio indicates greater excess return on the portfolio or asset and better performance relative to the risk taken. The formula is:

$$\text{IR} = \frac{R_p - R_a}{\sigma_{p-a}} \quad (18)$$

Where R_p denotes the portfolio return, R_a denotes the benchmark return, and σ_{p-a} denotes the standard deviation of the excess return.

3.6. *The TopKDropout Strategy*

The TopKDropout strategy emerges as a quantitative approach to stock selection, fundamentally rooted in the ranking of factor values. The strategy pivots on the selection of top-tier stocks based on their factor values, operating under the premise that these stocks are poised for superior performance in forthcoming periods. Distinctively, the TopKDropout strategy exclusively invests in the top k ranked stocks, eschewing those at the lower echelons of the ranking. By sporadically omitting certain high-attention positions from the self-attention weights, the strategy nudges the model towards gleaning insights from low-attention positions. Such an approach amplifies the portfolio’s concentration, curtails transactional overheads, and minimizes the inclusion of subop-

timal stocks, thereby bolstering the robustness and stability of the stock selection paradigm. The procedural breakdown of the TopKDropout strategy is as follows:

1. For the extant trading day, compute the factor values for each stock, contingent on a predefined set of factors.
2. Rank the stocks based on their factor value. Liquidate the 'Drop' stocks with the most diminutive predicted scores and acquire an equivalent number of other stocks with the zenithal predicted scores. An exception is made for the inception of the trade, ensuring a total of k stocks in possession.
3. Distribute funds equitably among the chosen stocks. Execute buying and selling operations in alignment with the trading frequency.
4. Upon the advent of the subsequent position-taking cycle, re-evaluate the factor values, select stocks, and iterate the aforementioned steps.

Figure 3 shows an example of a TopKDropout strategy.

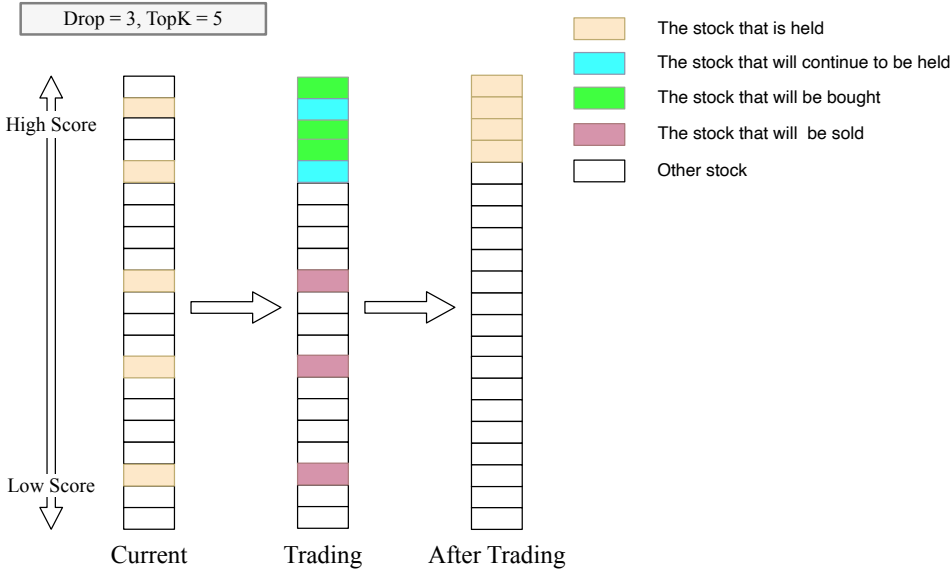


Figure 3: In the TopKDropout strategy, with TopK as 5 and Drop as 3: Prior to the subsequent position adjustment, the three lowest-ranked stocks are discarded. From the remaining stocks, excluding the current holdings, the top three with the highest scores (given by TopK-Drop, i.e., 5-3) are chosen for the next trading cycle.

4. Exploratory Data Analysis

4.1. Data Analysis and Preprocessing

In the course of our analysis, we discerned 15 salient variables related to stock characteristics that are crucial for factor construction. For example, the variable "rise" measures the percentage increase, typically spanning a range from [-10,10]. The term "zongshizhi" represents the Total Market Capitalization, which is computed from the product of a stock's market price and its total outstanding shares. The P/E Ratio, denoted as "shiyinglv", serves as a critical indicator of a stock's valuation. Collectively, these variables, among others, play a central role in predicting stock price movements.

Table 1: Key Stock-Related Variables for Factor Construction

Variable Name	Description	Remarks
code	Stock Code	6-character string
name	Stock Name	Total of 5108 stocks
rise	Increase	Generally fluctuates within the [-10,10] range
zhenfu	Amplitude	
lastclose	Last Close Price	T+1 period's last close price = T period's close price
open	Opening Price	
close	Closing Price	
high	Highest Price	
low	Lowest Price	
chengjiaogushu	Transaction Volume	Transaction Volume = Number of stocks sold + Number of stocks bought
chengjiaoe	Transaction Amount	Transaction Amount = Transaction Price \times Transaction Volume
zongshizhi	Total Market Value	Total Market Value = Stock Market Price \times Total Share Capital
zongguben	Total Share Capital	Includes restricted stocks and circulating stocks
shiyinglv	Price-to-Earnings Ratio	P/E Ratio = Stock Price Per Share / Earnings Per Share
shijinglv	Price-to-Book Ratio	P/B Ratio = Stock Price Per Share / Net Asset Value Per Share

Based on the classification of the US stock market exchanges and markets, a grouped bar chart was drawn. As shown in Figure 4, the New York Stock Exchange (NYSE), NASDAQ, the American Stock Exchange (AMEX), and Over-The-Counter (OTC). Notably, NASDAQ encompasses the largest number of stocks, totaling 3,673, while the OTC market comprises the least, with a mere

102 stocks. The AMEX primarily functions as a trading platform catering to small to medium-sized enterprises, and stocks listed here exhibit heightened volatility. In contrast, OTC stocks markedly differ from those on standard exchanges. To bolster the robustness of our ensuing stock predictions, our research and analysis focused predominantly on stocks from the NYSE and NASDAQ.

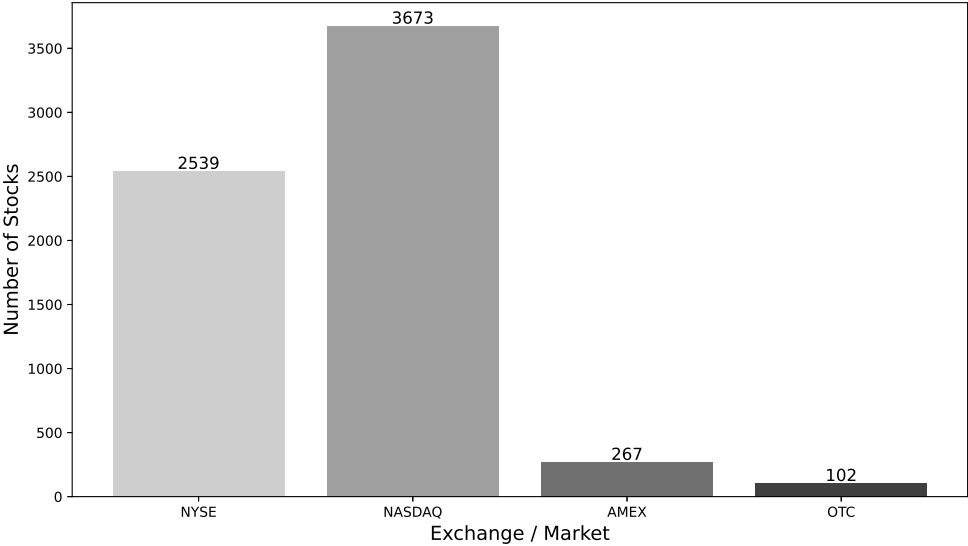


Figure 4: Distribution of Stocks Across Major US Stock Market Sectors

To provide an introductory insight into the overarching trend encapsulated within the dataset, we opted for the emblematic S&P 500 Index in the U.S. market, delineating the closing price trajectory from January 2020 through June 2023, as depicted in Figure 5. A discernible observation is the pronounced downward trend from January 2020 to March 2021, potentially exacerbated by the global pandemic. This observation underscored the necessity to integrate adjustments in our model to account for such exogenous events. A notable trough was reached on March 23, 2020, with the S&P 500 plummeting to a three-year nadir of 2,237.40. However, a resurgence was evident post-April 2020, culminating in a zenith of 4,796.56 on January 3, 2022, before a subsequent decline. The index then oscillated around the 4,000 threshold, mirroring the inherent volatility and intricacies of the securities market. Such dynamics accentuate the imperative of considering both the inherent rhythms of the stock market and the ramifications of unpredictable externalities, such as global pandemics.

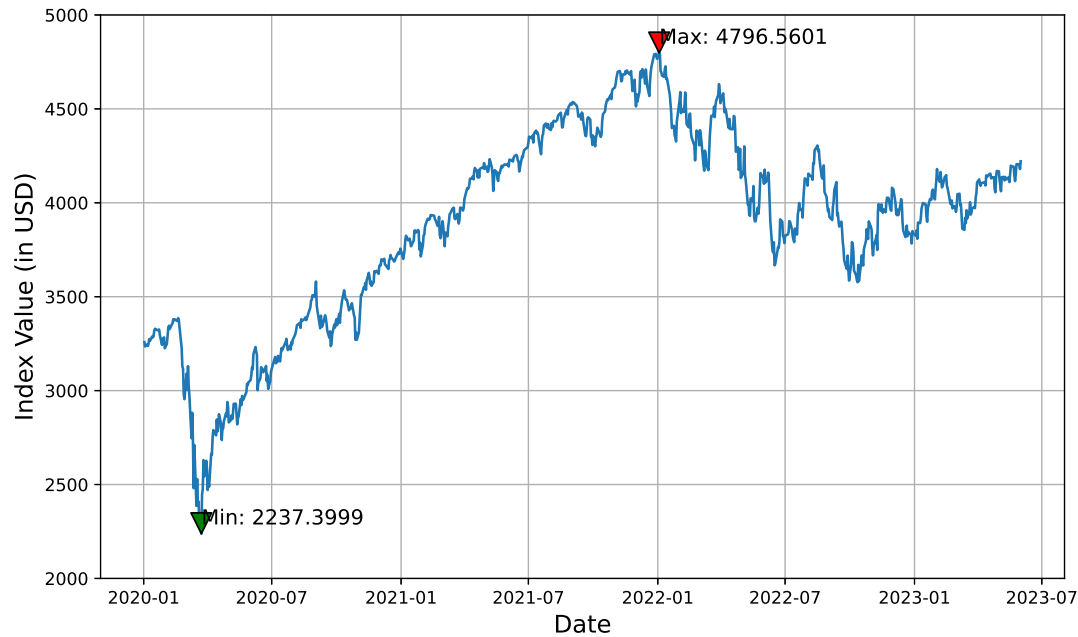


Figure 5: Trend of the S&P 500 Index from 2020 to June 2023

4.2. Stock Pool Construction

In our preliminary analysis of the U.S. stock market, the S&P 500 index emerged as the primary focus due to its comprehensive representation of the market landscape. The dataset, sourced from the iFinD terminal by Tonghuashun, encompasses financial and valuation metrics of the S&P 500 index stocks spanning from 2020 to the first half of 2023. For the purpose of model construction and validation, the period from January 2021 to January 2023 served as our training and validation set, while February 2023 to June 30, 2023, was designated as the test set.

The strategic selection of the S&P 500 as the stock pool is underpinned by its robust representativeness of the U.S. market. Comprising 500 of the most prominent publicly traded companies across a myriad of industries, the S&P 500 provides a panoramic view of market dynamics [Jiao & Jakubowicz \(2017\)](#). This expansive coverage not only ensures a holistic perspective but also guarantees a wealth of data, given the stature of the constituent companies. The transparency and abundance of financial and trading data available make it an invaluable resource for in-depth analysis [Gasparėnienė, Remeikiene, Sosidko & Vėbraitė \(2021\)](#). The S&P 500's global acclaim

has subjected it to rigorous academic and market evaluations, reinforcing its credibility as a foundational base for our machine learning model, thereby bolstering its precision and applicability [Krauss, Do & Huck \(2017\)](#); [Huotari, Savolainen & Collan \(2020\)](#). As illustrated in Figure 6, the distribution of industries within the S&P 500 is shown, highlighting the concentrations in sectors such as 'Industrials' and 'Information Technology'. Nevertheless, the S&P 500's inherent representativeness ensures a comprehensive inclusion of all pivotal industries, underscoring its broad universality [Kim, Han & Kim \(2022\)](#).

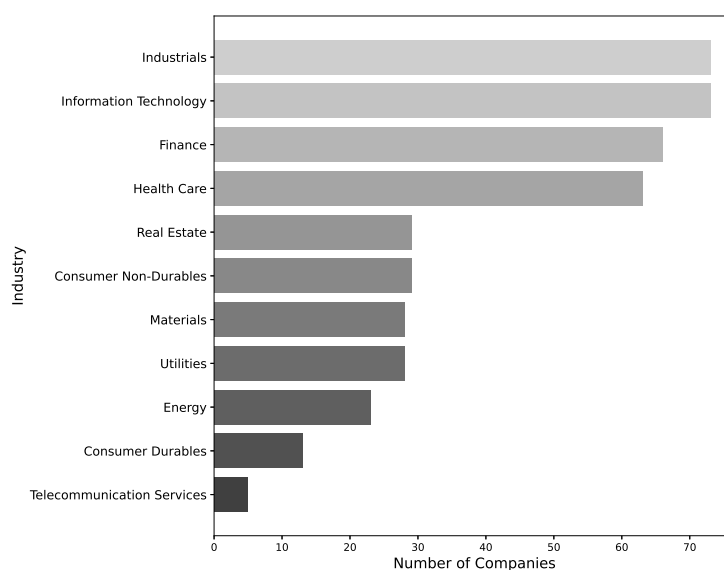


Figure 6: Industry Distribution of the S&P 500 Constituent Stocks

Furthermore, the application of deep learning techniques in predicting stock movements, especially within the S&P 500, has been gaining traction in recent years. Techniques such as deep neural networks, gradient-boosted trees, and random forests have been employed to exploit statistical arbitrage opportunities within the S&P 500, highlighting the index's significance in the realm of machine learning and finance [Krauss et al. \(2017\)](#); [Ding, Zhang, Liu & Duan \(2015\)](#). Additionally, the predictive power of machine learning, combined with technical analysis, has shown promise in outperforming traditional stock market prediction methods, further emphasizing the importance of our chosen stock pool [Macchiarulo \(2018\)](#).

5. Factor Pool Construction

5.1. Theoretical Foundation

The concept of factor-based stock selection can be traced back to the Capital Asset Pricing Model (CAPM) developed by Ross (1977). This model introduced a pivotal idea: under a set of assumptions, the overall market return can be used to depict the return of an individual asset (stock). The model is structured as shown in Equation 19:

$$r_i = r_f + \beta_{im}(r_m - r_f) + \mu_i \quad (19)$$

Where: r_i denotes the return of asset i , r_f represents the risk-free rate, β_{im} is the Beta coefficient, illustrating the systematic risk of asset i , and r_m is the overall return of market m , encompassing all stocks.

In this model, the overall market return can be perceived as an influencing factor for the return of any individual asset. This influence can be either positive or negative, mediated through the Beta coefficient. Consequently, CAPM is regarded as one of the earliest single-factor models. In contrast, multi-factor models extend beyond just market returns. They directly identify metrics correlated with stock returns for quantitative analysis, and based on this, construct stock portfolios to forecast future portfolio profit and loss. The inception of multi-factor models is widely believed to have been influenced by the Arbitrage Pricing Theory (APT). In the secondary stock market, a multi-factor model can be understood as decomposing the returns of N stocks into a linear combination of M factors and a residual term not explained by the factors, as illustrated in Equation 20:

$$r_i = \sum_{j=1}^M \beta_{ij} \times f_j + \mu_i \quad (20)$$

This can also be represented in vector form:

$$r = \beta f + \mu \quad (21)$$

Here, β_{ij} indicates the factor exposure of stock i on factor j , f_j represents the factor return, and μ_i is the residual return of stock i . As financial markets continue to evolve, using a linear combination to depict the relationship between factors and returns often falls short of real-world

demands. Therefore, there’s a need to adopt more advanced non-linear structures for description. However, factor construction remains an indispensable key step.

5.2. Factor Construction

This study is based on the Alpha158/Alpha360 factor library within the Qlib framework. In conjunction with relevant literature and research reports, we constructed a total of 158 short-term Alpha factors based on data such as price and trading volume. The data dimension for all these factors is daily trading data.

Table 2: Partial Factor Construction Methods

Factor Order	Factor Construction Method
...	...
Alpha5	$1/(T \text{ SMAX}(\text{CORR}(T \text{ SRANK}(\text{VOLUME}, 5), T \text{ SRANK}(\text{HIGH}, 5), 5), 3))$
Alpha6	$1/(\text{RANK}(\text{SIGN}(\text{DELTA}(\text{OPEN} * 0.85 + \text{HIGH} * 0.15), 4)))$
Alpha7	$(\text{RANK}(\text{MAX}(\text{VWAP} - \text{CLOSE}), 3)) + \dots$
Alpha8	$\text{RANK}(\text{DELTA}(1/(((\text{HIGH} + \text{LOW})/2) * 0.2) + (\text{VWAP} * 0.8)), 4))$
Alpha9	$\text{SMA}(((\text{HIGH} + \text{LOW})/2 - (\text{DELAY}(\text{HIGH}, 1) + \dots$
Alpha10	$(\text{RANK}(\text{MAX}(((\text{RET} ; 0) ? \text{STD}(\text{RET}, 20) : \text{CLOSE}) * 2), 5))$
...	...

Table 2 lists the construction methods of some of the factors, all of which belong to the volume-price factors. The construction methods for the remaining factors can be found in the appendix.

6. Experiments on Return Rate Model

This study conducted experiments to explore the Stockformer model and addressed the following three research questions:

Research Question 1. How should the cycles of STL time series decomposition be selected and determined for robustness?

Research Question 2. Does Stockformer outperform the baselines?

Research Question 3. How do different components of Stockformer (e.g., sequence decomposition methods, graph embeddings) impact its performance?

6.1. Experimental Setup

6.1.1. Dataset and Evaluation Metrics

The study took the return rates of the 500 stocks from the candidate pool, obtained in Section 5, and arranged them in a matrix format with dates as rows and individual stocks as columns, serving as the raw data input for wavelet decomposition. Based on the 158 factors constructed in Section 5, they were used as multi-factor inputs. The study used the actual return rates of the first 10 time steps to predict the return rates of the subsequent 2 time steps. These datasets were then divided into training (60%), validation (20%), and testing (20%) sets in chronological order. The performance of all methods was evaluated using three standard metrics: Mean Absolute Error (MAE), Mean Absolute Percentage Error (MAPE), and Root Mean Square Error (RMSE).

6.1.2. Baseline

In this study, the proposed model, Stockformer, is compared with the following benchmark models. Alongside the models introduced in the related work section, a total of 10 benchmark models are utilized for comparison:

1. LightGBM (Ke, Meng, Finley, Wang, Chen, Ma, Ye & Liu (2017)): An efficient distributed learning framework based on gradient boosting trees.
2. XGBoost (Chen & Guestrin (2016)): A gradient boosting tree model.
3. CatBoost (Dorogush, Ershov & Gulin (2018)): An ensemble learning model based on gradient boosting trees.
4. LSTM (Hochreiter & Schmidhuber (1997)): A Long Short-Term Memory network, a recurrent neural network model designed for handling sequential data.
5. GRU (Cho, Van Merriënboer, Gulcehre, Bahdanau, Bougares, Schwenk & Bengio (2014)): A Gated Recurrent Unit network, a recurrent neural network model for processing sequential data.
6. ALSTM (Wang & Hao (2020)): The Attention Long Short-Term Memory network is a variant of the LSTM neural network based on the attention mechanism. It selectively focuses on relevant information from the input sequence during prediction, enhancing the model's performance in sequential data tasks.
7. GAT (Velickovic, Cucurull, Casanova, Romero, Lio, Bengio et al. (2017)): The Graph Attention Network is a graph neural network model that employs attention mechanisms to learn

relationships between nodes and the weight of node features, enabling effective representation and prediction of graph data.

8. IGMTF (Xu, Liu, Bian, Yin & Liu (2021)): The Instance-based Graph Multivariate Time Series Forecasting framework is a graph-structured multivariate time series prediction model. By considering interconnections between different variables at different timestamps, it leverages historical time series information to predict target time series, achieving superior performance in multivariate time series forecasting compared to existing methods.
9. TCN (Bai, Kolter & Koltun (2018)): The Temporal Convolutional Network is a time series model based on convolutional neural networks. By employing one-dimensional convolution operations to extract local patterns and long-term dependencies in the time dimension, it offers efficient parallel computation capabilities and robust modeling capabilities, making it suitable for time series forecasting and sequence modeling tasks.
10. Localformer (Zheng, Zhou, Ye & Zhan (2023)): A model based on Hilbert flattening. By utilizing the Hilbert curve to unfold image matrices, it better preserves the smoothness of local information.

The replication of these baseline models and the subsequent Swing Strategy Backtesting for all models were conducted using Microsoft Research’s AI for quantitative investment platform, Qlib¹.

6.1.3. Parameter Configuration

In this study, the Stockformer model is implemented using the PyTorch framework and trained with the Adam optimizer for a total of 100 epochs. Due to computational resource constraints, the batch size for input data is set to 2. Within the Stockformer model, the number of heads e in the attention mechanism is set to 1, and the dimension d_e is set to 128. Additionally, the number of layers L in the spatiotemporal encoder is set to 2. To capture cyclical time dependencies, dilated causal convolutional layers with a kernel size of $J = 2$ are stacked. The initial learning rate is set to 0.001 and adjusted with a decay rate of 0.1. Dropout technique is also employed, setting the dropout rate to 0.2, to mitigate the risk of model overfitting.

¹Qlib: <https://github.com/microsoft/qlib>

6.2. Experimental Results

6.2.1. Determination of STL Time Series Decomposition Periodicity and Robustness (RQ 1)

Periodicity Determination. STL decomposition decomposes a time series into seasonal component S_t , trend component T_t , and residual component R_t . In this study, the Ljung-Box test is employed to determine the general periodicity of stock return series. Initially, stock return series are extracted from the time series data. Subsequently, each stock return series is decomposed using STL to obtain the seasonal, trend, and residual components. In this research, emphasis is placed on the residual component as it reflects random fluctuations in the series that are not explained by the trend and seasonality.

To determine the general periodicity of the stock return series, we select a period range starting from 2 and iterate to 100. For each period, the residuals of all stock return series post-STL decomposition are subjected to a ten-lag Ljung-Box test. A period is considered a reasonable return rate period if over 90% of the series residuals are white noise sequences.

Based on the Ljung-Box test results, we analyzed whether the ten-lag residuals of 90% of stock return series decomposed at each period passed the test. If the residuals pass the Ljung-Box test, it indicates that the residuals exhibit white noise characteristics, showing randomness or disorder, without evident periodicity or trend. This suggests that the seasonal and trend components at this period can characterize most of the return rate information.

Table 3: Ljung-Box Test Results

Lag Order	lb_stat	lb_pvalue
1	10.051	0.002
2	14.122	0.001
3	17.457	0.001
4	17.933	0.001
5	18.751	0.002
6	18.781	0.005
7	18.815	0.009
8	18.904	0.015
9	23.335	0.005
10	95.661	<0.001

After comparing the test results across different periods, we observed that over 90% of stock return series residuals significantly passed the Ljung-Box test at a period of 50 days (i.e., period =

50), being identified as white noise sequences. This period can be considered the general periodicity of the stock return series. The ten-lag Ljung-Box test results at this period (average of 500 stocks) are shown in Table 3.

Determination of Robustness. STL time series decomposition primarily has two decomposition methods: Robust and Non-Robust. The Robust decomposition is more robust when handling data with outliers or anomalies. By using weighted algorithms (like local weighted regression), Robust decomposition can reduce the impact of outliers on the decomposition results. In contrast, Non-Robust decomposition uses a simple averaging algorithm, is sensitive to outliers, and may be influenced by them. For a stock return series, the trend, seasonal, and residual components of Robust and Non-Robust STL decomposition are shown in Figure 7 (period=50, selected stock code is APPL.O).



Figure 7: Comparison of Trend, Seasonal, and Residual Components in Robust and Non-Robust STL Decomposition for Stock Return Series of APPL.O

From Figure 7, it can be observed that the trend component of Robust decomposition is smoother (less sensitive to outliers), while the trend component of Non-Robust decomposition exhibits more evident fluctuations. Observing the seasonal component, the Robust decomposi-

tion’s seasonal component fluctuates more, possibly because its trend component captures fewer fluctuations, failing to explain all the fluctuations in the data, making the seasonal component bear more volatility. In contrast, the Non-Robust decomposition’s trend component might better capture the data’s fluctuations, making its seasonal component’s volatility relatively smaller. Additionally, the residuals of Robust decomposition might have larger deviations, possibly because Robust decomposition is more robust to outliers, incorporating more outliers into the residuals, leading to increased deviations. In contrast, Non-Robust decomposition might be more influenced by outliers, fitting them better into the trend or seasonal components, resulting in smaller residuals.

Observing the results and interpretations, the Non-Robust STL decomposition method seems more appropriate as it is more sensitive to outliers, capturing the data’s fluctuations and changes more effectively.

To further determine which of the Robust and Non-Robust STL decompositions is better, we calculate the trend strength and seasonal strength of Robust and Non-Robust STL decompositions based on the measurement method in Section 3.1.2, to judge which decomposition method is stronger and more closely aligned with the original data’s fluctuations.

Table 4: Comparison of Trend Strength and Seasonal Strength

Decomposition Method	Trend Strength	Seasonal Strength
Non-Robust	0.023	0.425
Robust	0.002	0.114

Based on the results presented in Table 4, we can draw the following conclusions. Firstly, trend strength is an indicator measuring the importance of the trend component in the STL decomposition results. We observed that the trend strength of Non-Robust decomposition is 0.023, while that of Robust decomposition is 0.002. This indicates that Non-Robust decomposition has a better capability in capturing the long-term trend of the return rate series. Secondly, seasonal strength measures the importance of the seasonal component in the decomposition results. We noted that the seasonal strength of Non-Robust decomposition is 0.425, while that of Robust decomposition is 0.114. This indicates that Non-Robust decomposition has a stronger ability to capture the cyclical changes in the return rate series. In summary, the Non-Robust decomposition method exhibits better performance in capturing trend and seasonality, playing a significant role

in analyzing and interpreting stock return series.

6.2.2. Performance Comparison (RQ 2)

Table 5 showcases the performance of the proposed Stockformer model in comparison to state-of-the-art models using metrics such as MAE, RMSE, and MAPE.

Table 5: Comparison of Stockformer with State-of-the-Art Models

Model	MAE	RMSE	MAPE
LGBM	3.445	4.769	0.209
XGBoost	3.855	4.833	0.217
CATBoost	3.433	4.573	0.198
LSTM	2.546	3.552	0.372
GRU	2.348	3.357	1.075
ALSTM	2.302	3.254	0.855
GATs	2.033	3.080	0.368
IGMTF	3.069	4.120	0.346
TCN	1.829	3.044	0.357
Localformer	1.843	2.759	0.260
Stockformer	0.675	1.346	0.108

IGMTF essentially provides the lower bound of model performance. Machine learning methods (LGBM, XGBoost, and CATBoost) perform much worse than deep models, due to the nonlinear dependencies and the absence of handcrafted features. For all tasks, non-graph methods (such as LSTM and GRU) generally perform slightly worse than the graph-based benchmark methods like GATs, indicating the efficacy of graphs in modeling spatial dependencies. Localformer outperforms GATs, highlighting the effectiveness of the attention mechanism in modeling the dynamic interactions of stock returns. As one of the components in the Stockformer design, TCN performs better than the other models, suggesting that TCN captures the features of return rates more finely.

Overall, the Stockformer model excels in all metrics, achieving the lowest Mean Absolute Error (MAE) of 0.675, Root Mean Square Error (RMSE) of 1.346, and Mean Absolute Percentage Error (MAPE) of 0.108. This indicates that our model predicts stock returns with greater accuracy compared to other models.

Additionally, to gain a clearer understanding of the accuracy of the prediction of price movements, we also calculated the directional accuracy rate (i.e., the consistency of the predicted sign

of the return rate with the actual sign of the return rate). While the directional accuracy rate for the other ten models’ predictions of 500 stocks’ return rates hovers around 50%, the Stockformer model boasts a directional accuracy rate as high as 62.39%. The main reasons are:

1. Stockformer extracts trend and seasonal components from the stock return series and employs a bi-component encoder to model each component separately;
2. Stockformer adopts a fusion of attention and multi-supervision, effectively integrating and utilizing the information from the seasonal and trend components of the stock return series;
3. Stockformer introduces position encoding with the time graph and stock association graph, effectively capturing global dependencies and infusing structural information.

6.2.3. Ablation Study (RQ 3)

To investigate the effectiveness of different components of Stockformer, we compare it with six distinct variants:

1. "WSF (Wavelet Stockformer)": This variant employs the Discrete Wavelet Transform (DWT) instead of STL to decompose the stock return series.

Discrete Wavelet Transform. The Discrete Wavelet Transform (DWT) extracts low-frequency and high-frequency component sequences from the entangled flow layer of the return rate. The bi-component represents long-term and short-term time patterns. The low-frequency component is stable and has a long-term trend, representing the trajectory of the return rate. The high-frequency component, which is volatile, has short-term effects, representing sudden events in the stock market due to economic, political, and other influences. The DWT with input return rate series \mathcal{X} can be expressed as in Equation 22:

$$\bar{\mathcal{X}}_l = \mathbf{g}\mathcal{X}, \bar{\mathcal{X}}_h = \mathbf{h}\mathcal{X}, \quad (22)$$

Where the candidate low-frequency and high-frequency components $\bar{\mathcal{X}}_l$ and $\bar{\mathcal{X}}_h$ have their time steps reduced to half of the input due to the downsampling operation in DWT. Therefore, this layer up-samples the input using inverse low-pass and high-pass filters $\mathbf{g}^T, \mathbf{h}^T$. The 360-dimensional multi-factor features are then concatenated with the up-sampled low-frequency and high-frequency components, respectively, to obtain the final multi-dimensional

low-frequency and high-frequency inputs. A fully connected layer then transforms the low-frequency and high-frequency components into high-dimensional $\mathcal{X}_l, \mathcal{X}_h \in \mathbb{R}^{T_1 \times N \times d}$. The upsampling operation and the fully connected layer are formalized in Equation 23:

$$\mathcal{X}_l = W^g \mathbf{g}^T \bar{\mathcal{X}}_l + b^g, \mathcal{X}_h = W^h \mathbf{h}^T \bar{\mathcal{X}}_h + b^h, \quad (23)$$

Where $W^g, W^h \in \mathbb{R}^{C \times d}$ and $b^g, b^h \in \mathbb{R}^d$ are learnable parameters.

2. "w/o MS (Multi-Supervision)": Stockformer without multi-supervision.
3. "w/o DL (Decoupling Flow Layer)": Stockformer without the decoupling flow layer.
4. "w/o F": Stockformer where fusion attention is replaced with an addition operation.
5. "w/o DT (Dilated causal convolution and Temporal Attention)": Stockformer without dilated causal convolution and temporal attention.
6. "w/o G": Stockformer without temporal slots and Struc2Vec graph attention.

Table 6: Ablation Study Results for Exports

Model	MAE	RMSE	MAPE
WSF	1.732	2.673	0.123
Stockformer-w/o MS	1.998	3.234	0.208
Stockformer-w/o DL	2.145	3.551	0.342
Stockformer-w/o F	2.435	3.062	0.325
Stockformer-w/o DT	2.758	3.875	0.358
Stockformer-w/o G	2.943	4.754	0.547
Stockformer	0.675	1.346	0.108

Table 6 displays the comparison results. It's evident that the full version of Stockformer outperforms the variants.

The WSF variant, utilizing the Discrete Wavelet Transform for stock return series decomposition, performs similarly to Stockformer but falls short. This shortfall might arise from the DWT process, which reduces the time step and requires upsampling, potentially losing some sequence information. Conversely, the STL decomposition maintains the original sequence length, giving Stockformer an edge. The more significant performance decline in "w/o G" compared to "w/o DT" highlights the spatial dimension's importance in the model, especially with the integration of temporal slots and Struc2Vec graph attention in Stockformer. The subpar performance of "w/o

DL”, ”w/o F”, and ”w/o MS” models can be attributed to changes in fusion attention, the omission of the decoupling flow layer, and the absence of multi-supervision. These elements are crucial for the model’s information processing and pattern recognition capabilities. In essence, Stockformer’s strength lies in its six carefully crafted components.

7. Swing Strategy Backtesting

Swing trading is a strategy that aims to capture gains in a stock within an intermediate time frame, typically from a few days to several weeks. This strategy is predicated on the identification of ’swings’ in stock prices, which are significant fluctuations that occur due to market volatility. Swing traders utilize technical analysis to find stocks with short-term price momentum and often combine this with fundamental analysis to confirm the trend.

The essence of swing trading lies in the trader’s ability to capitalize on the natural ebb and flow of stock prices, taking advantage of the momentum in the direction of the trend until it shows signs of reversal. The strategy requires a keen understanding of market trends, technical indicators, and stock performance patterns.

In the context of this study, the model’s forecasted return rate is leveraged as a unique factor to establish a testing model tailored for the swing trading strategy. The backtesting methodology, a pivotal element in the validation of trading strategies, is meticulously structured as follows:

Backtesting is the process of simulating a trading strategy using historical market data to determine its feasibility and prospective profitability. This critical evaluation allows traders to fine-tune their strategies in a controlled environment prior to real-world implementation. The backtesting procedure encompasses the following pivotal steps:

1. **Selection of Stock Pool:** The study utilizes a carefully curated selection of U.S. stocks, ensuring a robust and representative sample for analysis.
2. **Backtesting Period:** The temporal scope of the backtesting extends from February 1, 2023, to June 30, 2023, providing a substantial interval to assess the strategy’s performance.
3. **Data Handling:** The anticipated returns of stocks, as projected by the model, are harnessed as the sole factor in this analysis. Stocks that lack associated factor values are systematically excluded from the subsequent stratification process.

4. **Stratification Methodology:** Each trading day, the stocks within the pool are organized in ascending order based on their factor values. This ranking is then used to divide the pool into quintiles. The returns of each quintile are meticulously calculated for every trading day, facilitating a granular analysis of the strategy's effectiveness across different market segments.

This backtesting framework is designed to rigorously test the swing trading strategy, providing insights into the model's ability to predict returns and optimize the timing for market entry and exit, thereby aiming to maximize investment returns.

7.1. Factor Validity Test

7.1.1. IC Value Analysis

From the methodological discourse delineated earlier, the IC value inherently lies between -1 and 1. An IC value less than 0 signifies a negative correlation between the predicted and actual stock returns. This suggests that during periods of actual positive returns, the strategy incurs negative returns, indicating suboptimal performance. Conversely, an IC value greater than 0 indicates a positive correlation, signifying that the strategy is yielding favorable outcomes. Thus, a stock selection strategy of high caliber and minimal error should manifest a substantially large IC value.

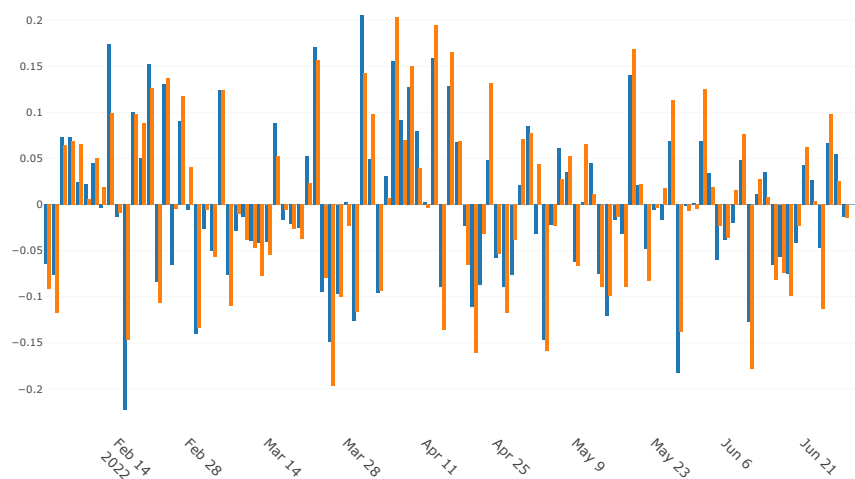


Figure 8: IC values from February 1, 2023 to June 30, 2023

Considering the predicted return rate as an isolated factor and juxtaposing it with the actual return IC value, as illustrated in the subsequent Figure 8, the IC values spanning from February 1, 2023, to June 30, 2023, are presented. The conventional IC values are derived using the Pearson correlation coefficient, while the Rank IC values employ the Spearman correlation coefficient. The aggregate IC value fluctuates between -0.15 and 0.2. An IC exceeding 0.05 is indicative of an efficacious factor. Moreover, an IC surpassing 0.1 can serve as a robust stock selection criterion, aptly reflecting stock trend nuances. Consequently, the model's outcomes are commendably satisfactory.

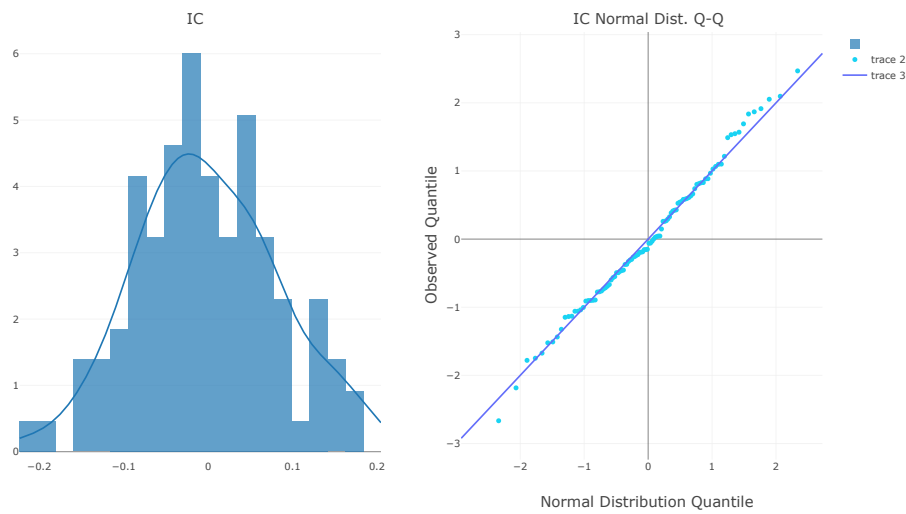


Figure 9: Distribution of IC Values and Q-Q Plot for Normality Assessment

Subsequent to this, an exploration concerning the IC value distribution is undertaken. Figure 9 delineates the IC value distribution histogram and the Q-Q plot pertinent to the distribution normality test. In the leftmost illustration, the IC value approximates a bell-curve distribution with a mean value exceeding 0. The rightmost diagram showcases the majority of data points aligning along a 45-degree straight line, signifying that the IC value adheres to a normal distribution with a mean of 1.

As depicted in Figure 10, an analysis of the IC values from February to June 2023 reveals a range predominantly between -0.01 and 0.02, showcasing relative stability. The IC values during February and April peaked at approximately 0.02, while May witnessed the nadir at close to -0.01.

Collating the intrinsic characteristics of the aforementioned IC values, it becomes evident that

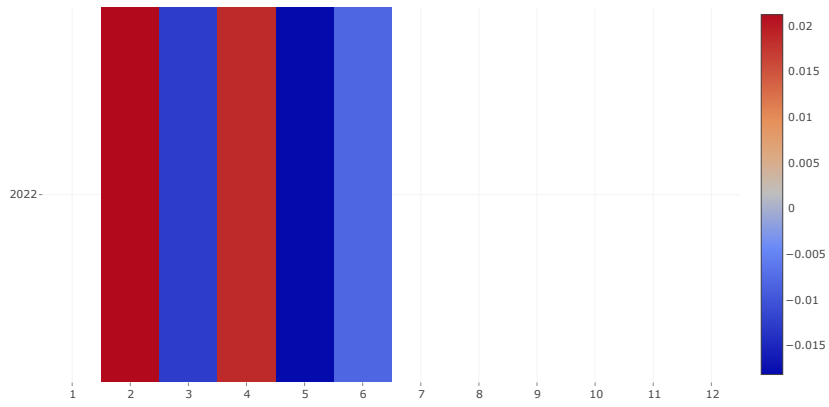


Figure 10: Distribution of Monthly IC Values

when the model's yield prediction is analyzed as a singular factor against the genuine yield, an overarching IC value surpassing 0.02 is achieved, underscoring its efficacy as a factor.

7.1.2. Layered Backtesting Analysis of Predicted Return Rate

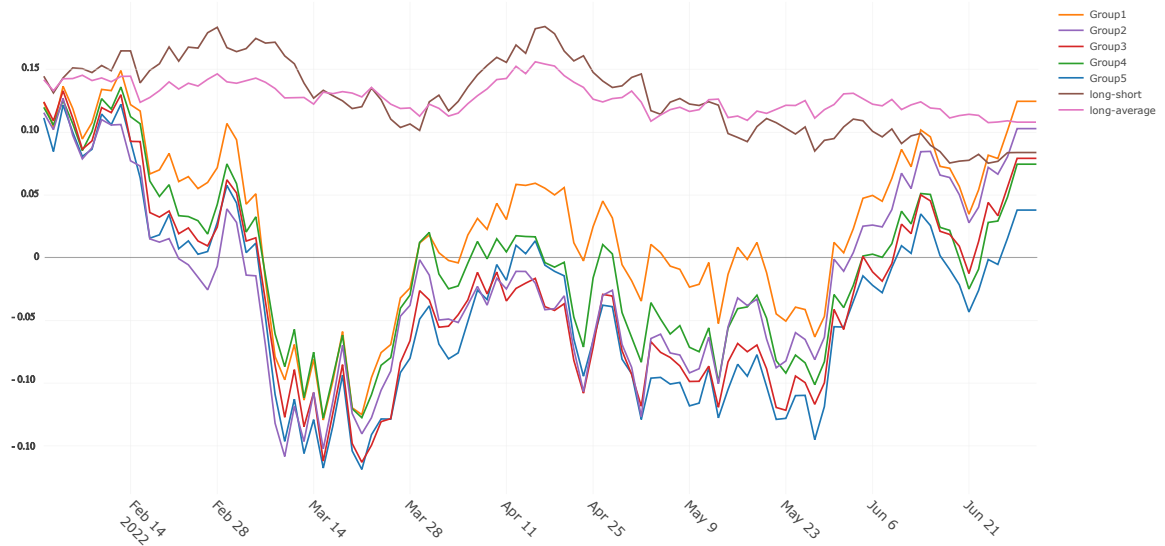


Figure 11: Layered Backtesting of Cumulative Investment Returns (February to June 2023)

This study considers the model's predicted return rate as a single factor to test the model, with the construction methodology for the testing model being:

1. The stock pool consists of stocks from the S&P 500;
2. The backtesting period: February 1, 2023, to June 30, 2023; the portfolio is rebalanced daily;
3. Data processing: The model's predicted stock return rates are treated as a single factor, and stocks without factor values are excluded from the layering;
4. Layering method: On each trading day, stocks are sorted in descending order based on the factor value (predicted stock return), and the stock pool is equally divided into 5 groups named Group1 to Group5. The return of each stock pool is then calculated for each trading day.

Figure 11 elucidates the cumulative returns of five segregated equity portfolios from February to June 2023. There is a sequential augmentation of cumulative returns from Group 5 to Group 1, with Group 1 almost reaching a 15% return rate. This gradient of increasing returns indicates that the single factor derived from the model is imbued with robust monotonicity, which speaks to the model's effectiveness.

In examining long-term trend strategies, both the long-short and long-average strategies have maintained relatively stable oscillations at a higher level throughout the duration in question. The long-short strategy, indicated by the brown line, and the long-average strategy, marked by the pink line, demonstrate a steadiness in performance, suggesting a degree of resilience against market volatility.

This analysis underscores the model's adeptness at constructing a factor with solid monotonic characteristics. Moreover, the consistent high-level fluctuations of the long-short and long-average strategies underscore their strategic reliability and potential for risk-adjusted outperformance over the analyzed timeframe.

7.2. Backtesting and Performance Analysis

7.2.1. Backtesting Parameter Settings

In this study, we conduct a comprehensive backtest of the proposed strategy, setting the parameters as delineated below:

1. The backtesting duration spans from 2023-02-01 to 2023-06-30.

2. We employ the TopKDropout strategy for trading, with the parameters Topk and Drop set to 10 and 2, respectively.
3. The transaction volume is set at \$100,000, with daily transaction frequency.
4. The S&P500 index serves as the benchmark for comparison.
5. We utilize the stock pool curated in prior sections of this paper.
6. Taking into account the commission fees, regulatory fees, and trade execution expenses, the total cost of trading in the U.S. stock market is structured with a baseline minimum cost of \$5 per transaction.
7. Transactions are simulated using the closing prices, excluding stocks with trading halts or price limits.

7.2.2. Backtesting Result Analysis

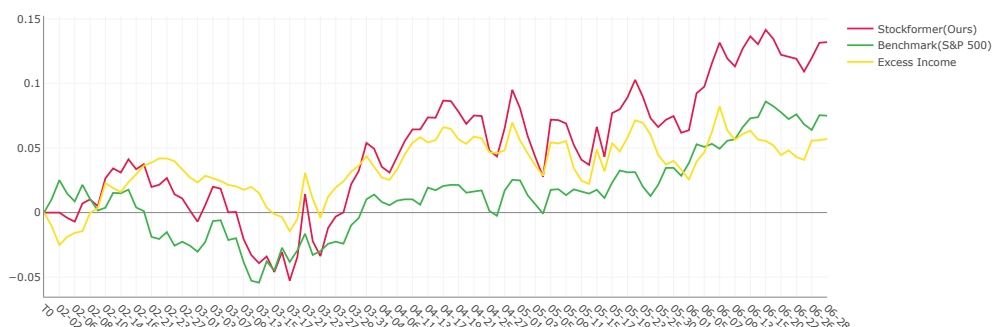


Figure 12: Cumulative Return Curve for the TopKDropout Strategy From February to June 2023.

The Figure 12 presents three distinct curves, each representing a different aspect of the trading analysis. The red line illustrates the cumulative returns of the TopkDropout Swing trading strategy, which is based on the Stockformer’s predicted returns. The green line depicts the cumulative returns of the S&P 500 index, serving as a benchmark for market performance. The yellow line indicates the strategy’s excess returns over the benchmark.

From February 1, 2023, to June 28, 2023, the TopkDropout Swing trading strategy achieved a cumulative return of 13.19%, with an excess return of approximately 5.69%. During the entire month of February, the broader market exhibited a downward trend. Although the strategy showed a brief period of underperformance—where the cumulative returns of the trading strategy fell short of the S&P 500 index—it still managed to secure a substantial excess return overall. Following

March, as the market trend shifted to an upward trajectory, the strategy’s returns closely mirrored the rising market, consistently outperforming the S&P 500 index and ultimately securing a higher excess return by June. This performance underscores the Stockformer model’s adeptness at forecasting the return rate for $t + 2$ timeframes, affirming its competence in backtesting the swing trading strategy.

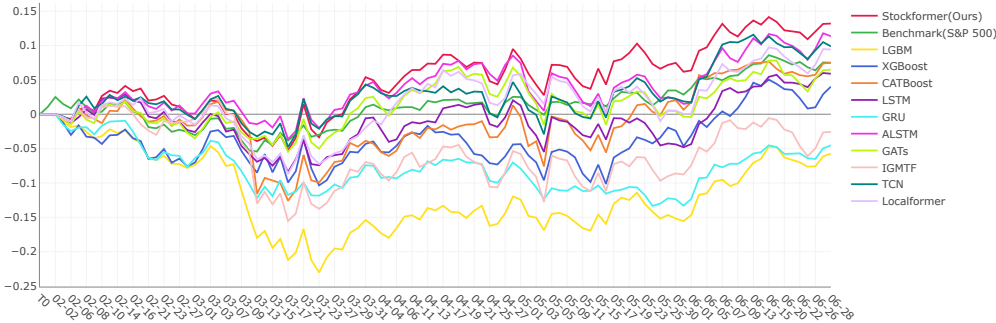


Figure 13: Cumulative returns of different models from February to June 2023.

In order to elucidate the substantial advantage we have achieved in the backtesting of our swing strategy, we continue to compare the cumulative return rates of the ten models discussed in the previous chapters, employing the same TopkDropout Swing trading strategy. As illustrated in Figure 13, it is evident that, compared to other advanced predictive models, Stockformer’s cumulative return rate is significantly higher. From February 1, 2023, to June 28, 2023, the cumulative return was 13.19%, closely followed by ALSTM with a cumulative return of 11.36%. This underscores the significant impact of the introduction of the self-attention mechanism on the model’s predictive capabilities. Subsequently, the TCN model exhibits a cumulative return rate of 9.88%. Notably, TCN is an integral component of our Stockformer model, which indirectly reflects the importance of incorporating this component in the prediction of return rates and the swing strategy. The cumulative return rate for Localformer is 9.42%. As a variant of the Transformer, which our Stockformer is also based upon, it demonstrates that our model has inherited the robust attributes of the Transformer. For a clearer comparison of the performance of each model, detailed information is provided in the table below.

Table 7 presents a compelling narrative of the predictive prowess of the Stockformer model. With a semi-annual cumulative return rate of 32.61% and an annualized return rate of 30.80%, Stockformer not only outperforms its SOTA but also demonstrates a robust resilience with a

Table 7: Comparative Analysis of Semi-Annual and Annualized Returns Across Predictive Models

Model	Semi-annual Cumulative Return Rate	Annualized Return Rate	Maximum Drawdown	Information Ratio
LGBM	-14.18%	-13.40%	-23.03%	-0.58
XGBoost	9.90%	9.34%	-10.36%	0.37
CATBoost	18.46%	17.43%	-14.81%	0.59
LSTM	14.57%	13.76%	-11.31%	0.62
GRU	-11.21%	-10.58%	-13.35%	-0.62
ALSTM	28.07%	26.51%	-8.45%	1.10
GATs	16.03%	15.13%	-8.48%	0.66
IGMTF	-6.35%	-6.00%	-17.78%	-0.20
TCN	24.42%	23.07%	-7.60%	0.97
Localformer	23.27%	21.98%	-10.99%	0.95
Stockformer	32.61%	30.80%	-9.39%	1.34

maximum drawdown of -9.39%. The information ratio of 1.34 further attests to its superior risk-adjusted returns. The ALSTM model, with the lowest maximum drawdown, indicates a strong defensive mechanism against market downturns. However, the Stockformer’s balanced approach to achieving high returns while maintaining a relatively low drawdown showcases its effectiveness in the swing trading strategy. The performance of the TCN and Localformer models also reflects the strength of components derived from the Transformer architecture, reinforcing the Stockformer’s architectural choices. This analysis not only highlights the success of the Stockformer but also validates the strategic integration of its components, which are pivotal in enhancing the model’s forecasting accuracy and, by extension, the profitability of the swing trading strategy.

8. Conclusion and Future Work

Conclusion. In grappling with the unpredictable nature of the securities market, we have crafted a deep learning construct termed ‘Swing Trading Strategy Based on STL Decomposition and Self-Attention Networks (Stockformer).’ By mining the S&P 500 index and detailed corporate financials, we’ve curated a selection pool of 500 stocks, underpinned by 158 price-volume factors (Alpha 158), each grounded in empirical industry analyses and academic discourse. The pioneering use of STL decomposition on stock return rates permits a granular dissection into seasonal, trend, and residual elements, later fused with chosen factors. A dual-component spatiotemporal encoder adeptly traces temporal correlations, complemented by Struc2Vec’s grasp on structural

intricacies within stock return data. The decoding stage employs fusion attention and multiple supervisory facets to synthesize trend and seasonal data, thereby refining the forecasting mechanism. Our empirical trials yield a commendable predictive accuracy of 62.39% for stock return rates—an auspicious feat amidst the stock market’s capricious nature. Additionally, the Stockformer’s performance, during the February to June 2023 backtesting phase, registered a cumulative return of 13.19% and an annualized return of 30.80%, markedly outstripping existing benchmarks. These results illuminate Stockformer’s profound predictive potential.

Future Work. Despite the strides made with Stockformer, future research beckons for further refinement. Presently, determining STL decomposition’s periodicity involves scrutinizing the residual for stochasticity—a task both laborious and iterative. Upcoming iterations will aim to encapsulate periodicity within the neural framework, enabling the model to autonomously pinpoint optimal periodic values, thus streamlining preliminary data analysis efforts. Moreover, the S&P 500 Index’s stock roster is inherently dynamic, and anchoring our model to a fixed stock pool could culminate in a suboptimal trading substrate. We’re thus poised to explore dynamic updating mechanisms for the stock pool to sharpen our predictive acumen. Additionally, to counter the introduction of new stocks—which may challenge our model’s established parameters—we envisage incorporating meta-learning paradigms to enhance the model’s adaptability, ensuring Stockformer retains its analytical acumen across novel scenarios.

Acknowledgements

Thank people. List funding agencies. Comment this section out if it reveals the authors’ identities.

References

- Aboussalah, A., Xu, Z., & Lee, C.-G. (2021). What is the value of the cross-sectional approach to deep reinforcement learning? *Quantitative Finance*, 21, 1239–1256. doi:[10.1080/14697688.2021.2001032](https://doi.org/10.1080/14697688.2021.2001032).
- Bai, S., Kolter, J. Z., & Koltun, V. (2018). An empirical evaluation of generic convolutional and recurrent networks for sequence modeling. *arXiv preprint arXiv:1803.01271*, . doi:[10.48550/arXiv.1803.01271](https://doi.org/10.48550/arXiv.1803.01271).
- Bonizzi, P., Karel, J. M., Meste, O., & Peeters, R. (2014). Singular spectrum decomposition: a new method for time series decomposition. *Advances in Adaptive Data Analysis*, 6, 1450011. doi:[10.1142/S1793536914500113](https://doi.org/10.1142/S1793536914500113).
- Chan, E. P. (2021). *Quantitative trading: how to build your own algorithmic trading business*. John Wiley & Sons.

- Chen, G., & Wang, Z.-C. (2012). A signal decomposition theorem with hilbert transform and its application to narrowband time series with closely spaced frequency components. *Mechanical Systems and Signal Processing*, 28, 258–279. doi:[10.1016/J.YMSSP.2011.02.002](https://doi.org/10.1016/J.YMSSP.2011.02.002).
- Chen, T., & Guestrin, C. (2016). Xgboost: A scalable tree boosting system. In *Proceedings of the 22nd acm sigkdd international conference on knowledge discovery and data mining* (pp. 785–794). doi:[10.1145/2939672.2939785](https://doi.org/10.1145/2939672.2939785).
- Cho, K., Van Merriënboer, B., Gulcehre, C., Bahdanau, D., Bougares, F., Schwenk, H., & Bengio, Y. (2014). Learning phrase representations using rnn encoder-decoder for statistical machine translation. *arXiv preprint arXiv:1406.1078*, . doi:[10.48550/arXiv.1406.1078](https://doi.org/10.48550/arXiv.1406.1078).
- Cleveland, R. B., Cleveland, W. S., McRae, J. E., & Terpenning, I. (1990). Stl: A seasonal-trend decomposition procedure based on loess. *Journal of Official Statistics*, 6, 3.
- Dagum, E. B., & Bianconcini, S. (2016). *Seasonal adjustment methods and real time trend-cycle estimation*. Springer. doi:[10.1007/978-3-319-31822-6](https://doi.org/10.1007/978-3-319-31822-6).
- De Prado, M. L. (2018). *Advances in financial machine learning*. John Wiley & Sons.
- Ding, X., Zhang, Y., Liu, T., & Duan, J. (2015). Deep learning for event-driven stock prediction. In *Twenty-fourth international joint conference on artificial intelligence*. doi:[10.5555/2832415.2832572](https://doi.org/10.5555/2832415.2832572).
- Dorogush, A. V., Ershov, V., & Gulin, A. (2018). Catboost: gradient boosting with categorical features support. *arXiv preprint arXiv:1810.11363*, . doi:[10.48550/arXiv.1810.11363](https://doi.org/10.48550/arXiv.1810.11363).
- Fama, E. F., & French, K. R. (1992). The cross-section of expected stock returns. *the Journal of Finance*, 47, 427–465. doi:[10.2139/ssrn.2511246](https://doi.org/10.2139/ssrn.2511246).
- Fama, E. F., & French, K. R. (2015). A five-factor asset pricing model. *Journal of financial economics*, 116, 1–22. doi:[10.1016/j.jfineco.2014.10.010](https://doi.org/10.1016/j.jfineco.2014.10.010).
- Fang, Y., Qin, Y., Luo, H., Zhao, F., Xu, B., Wang, C., & Zeng, L. (2021). Spatio-temporal meets wavelet: Disentangled traffic flow forecasting via efficient spectral graph attention network. *arXiv e-prints*, (pp. arXiv–2112). doi:[10.48550/arXiv.2112.02740](https://doi.org/10.48550/arXiv.2112.02740).
- Fung, W., & Hsieh, D. A. (1997). Empirical characteristics of dynamic trading strategies: The case of hedge funds. *The review of financial studies*, 10, 275–302. doi:[10.1093/rfs/10.2.275](https://doi.org/10.1093/rfs/10.2.275).
- Gasparénienė, L., Remeikiene, R., Sosidko, A., & Vėbraitė, V. (2021). A modelling of s&p 500 index price based on us economic indicators: Machine learning approach. *Engineering Economics*, 32, 362–375. doi:[10.5755/j01.ee.32.4.27985](https://doi.org/10.5755/j01.ee.32.4.27985).
- Georgakopoulos, H. (2015). *Quantitative trading with R: understanding mathematical and computational tools from a quant's perspective*. Springer.
- Green, J., Hand, J. R., & Zhang, X. F. (2017). The characteristics that provide independent information about average us monthly stock returns. *The Review of Financial Studies*, 30, 4389–4436. doi:[10.2139/ssrn.2262374](https://doi.org/10.2139/ssrn.2262374).
- Guo, J., Wang, S., Ni, L., & Shum, H. (2022). Quant 4.0: Engineering quantitative investment with automated, explainable and knowledge-driven artificial intelligence. *arXiv preprint arXiv:2301.04020*, . URL: <http://arxiv.org/pdf/2301.04020>. doi:[10.48550/arXiv.2301.04020](https://doi.org/10.48550/arXiv.2301.04020).
- Hochreiter, S., & Schmidhuber, J. (1997). Long short-term memory. *Neural computation*, 9, 1735–1780. doi:[10.1162/neco.1997.9.8.1735](https://doi.org/10.1162/neco.1997.9.8.1735).

- Huang, L., Cai, T., Feng, S., & Xie, Z. (2023). Quantitative trading strategy based on simplified dpg. *Healthcare Bulletin of Economics and Management*, 13, 8616. URL: <https://drpress.org/ojs/index.php/HBEM/article/download/8616/8386>. doi:10.54097/hbem.v13i.8616.
- Huang, N., Shen, Z., Long, S., Wu, M. C., Shih, H. H., Zheng, Q., Yen, N., Tung, C., & Liu, H. H. (1998). The empirical mode decomposition and the hilbert spectrum for nonlinear and non-stationary time series analysis. *Proceedings of the Royal Society of London. Series A: Mathematical, Physical and Engineering Sciences*, 454, 903–995. doi:10.1098/rspa.1998.0193.
- Huotari, T., Savolainen, J., & Collan, M. (2020). Deep reinforcement learning agent for s&p 500 stock selection. *Axioms*, 9, 130. doi:10.3390/axioms9040130.
- Jiao, Y., & Jakubowicz, J. (2017). Predicting stock movement direction with machine learning: An extensive study on s&p 500 stocks. In *2017 IEEE International Conference on Big Data (Big Data)* (pp. 4705–4713). IEEE. doi:10.1109/BigData.2017.8258518.
- Ke, G., Meng, Q., Finley, T., Wang, T., Chen, W., Ma, W., Ye, Q., & Liu, T.-Y. (2017). Lightgbm: A highly efficient gradient boosting decision tree. *Advances in neural information processing systems*, 30. doi:10.5555/3294996.3295074.
- Kim, J. M., Han, H. H., & Kim, S. (2022). Forecasting crude oil prices with major s&p 500 stock prices: Deep learning, gaussian process, and vine copula. *Axioms*, 11, 375. doi:10.3390/axioms11080375.
- Krauss, C., Do, X. A., & Huck, N. (2017). Deep neural networks, gradient-boosted trees, random forests: Statistical arbitrage on the s&p 500. *European Journal of Operational Research*, 259, 689–702. doi:10.1016/j.ejor.2016.10.031.
- Li, W., Hu, C., & Luo, Y. (2023). A deep learning approach with extensive sentiment analysis for quantitative investment. *Electronics*, 12. doi:10.3390/electronics12183960. [Online]. Available: <https://www.mdpi.com/2079-9292/12/18/3960>.
- Li, Y., Fu, K., Wang, Z., Shahabi, C., Ye, J., & Liu, Y. (2018). Multi-task representation learning for travel time estimation. In *Proceedings of the 24th ACM SIGKDD international conference on knowledge discovery & data mining* (pp. 1695–1704). doi:10.1145/3219819.3220033.
- Macchiarulo, A. (2018). Predicting and beating the stock market with machine learning and technical analysis. *Journal of Internet Banking and Commerce*, 23, 1–22. URL: <https://api.semanticscholar.org/CorpusID:158446761>.
- Providence, A. M., Yang, C., Orphe, T. B., Mabaire, A., & Agordzo, G. K. (2022). Spatial and temporal normalization for multi-variate time series prediction using machine learning algorithms. *Electronics*, 11, 3167. doi:10.3390/electronics111931676.
- Qian, E. E., Hua, R. H., & Sorensen, E. H. (2007). *Quantitative equity portfolio management: modern techniques and applications*. CRC Press.
- Qian, X.-Y., & Gao, S. (2017). Financial series prediction: Comparison between precision of time series models and machine learning methods. *arXiv preprint arXiv:1706.00948*, . doi:10.48550/arXiv.1706.00948.
- Ribeiro, L. F., Saverese, P. H., & Figueiredo, D. R. (2017). struc2vec: Learning node representations from structural identity. In *Proceedings of the 23rd ACM SIGKDD international conference on knowledge discovery and data*

- mining (pp. 385–394). doi:[10.1145/3097983.3098061](https://doi.org/10.1145/3097983.3098061).
- Ross, S. (1977). The capital asset pricing model (capm), short-sale restrictions and related issues. *The Journal of Finance*, *32*, 177–183. URL: <https://dx.doi.org/10.1111/J.1540-6261.1977.TB03251.X>. doi:[10.1111/J.1540-6261.1977.TB03251.X](https://doi.org/10.1111/J.1540-6261.1977.TB03251.X).
- Ruan, T., Lei, L., Zhou, Y., Zhai, J., Zhang, L., He, P., & Gao, J. (2019). Representation learning for clinical time series prediction tasks in electronic health records. *BMC Medical Informatics and Decision Making*, *19*, 1–12. doi:[10.1109/bibm.2018.8621136](https://doi.org/10.1109/bibm.2018.8621136).
- Singh, P. (2018). Novel fourier quadrature transforms and analytic signal representations for nonlinear and non-stationary time-series analysis. *Royal Society open science*, *5*, 181131. doi:[10.1098/rsos.181131](https://doi.org/10.1098/rsos.181131).
- Velickovic, P., Cucurull, G., Casanova, A., Romero, A., Lio, P., Bengio, Y. et al. (2017). Graph attention networks. *stat*, *1050*, 10–48550. doi:[10.17863/CAM.48429](https://doi.org/10.17863/CAM.48429).
- Wang, J., Zhuang, Z., & Feng, L. (2022). Intelligent optimization based multi-factor deep learning stock selection model and quantitative trading strategy. *Mathematics*, *10*. doi:[10.3390/math10040566](https://doi.org/10.3390/math10040566). [Online]. Available: <https://www.mdpi.com/2227-7390/10/4/566>.
- Wang, Q., & Hao, Y. (2020). Alstm: An attention-based long short-term memory framework for knowledge base reasoning. *Neurocomputing*, *399*, 342–351. doi:[10.1016/j.neucom.2020.02.065](https://doi.org/10.1016/j.neucom.2020.02.065).
- Wang, X., Smith, K., & Hyndman, R. (2006). Characteristic-based clustering for time series data. *Data mining and knowledge Discovery*, *13*, 335–364. doi:[10.1007/s10618-005-0039-x](https://doi.org/10.1007/s10618-005-0039-x).
- Wang, Y., & Huang, S. (2022). Research on quantitative investment strategies based on deep learning algorithms in the context of the need for information management. In *2022 IEEE International Conference on Industrial Management (ICIM)*. IEEE. doi:[10.1109/ICIM56520.2022.00048](https://doi.org/10.1109/ICIM56520.2022.00048) [Online]. Available: <https://dx.doi.org/10.1109/ICIM56520.2022.00048>.
- Xu, W., Liu, W., Bian, J., Yin, J., & Liu, T.-Y. (2021). Instance-wise graph-based framework for multivariate time series forecasting. *arXiv preprint arXiv:2109.06489*, . doi:[10.48550/arXiv.2109.06489](https://doi.org/10.48550/arXiv.2109.06489).
- Yuan, H., Li, G., Bao, Z., & Feng, L. (2020). Effective travel time estimation: When historical trajectories over road networks matter. In *Proceedings of the 2020 acm sigmod international conference on management of data* (pp. 2135–2149). doi:[10.1145/3318464.3389771](https://doi.org/10.1145/3318464.3389771).
- Yue, H., Liu, J., & Zhang, Q. (2022). Applications of markov decision process model and deep learning in quantitative portfolio management during the covid-19 pandemic. *Systems*, *10*, 146. URL: <https://www.mdpi.com/2079-8954/10/5/146>. doi:[10.3390/systems10050146](https://doi.org/10.3390/systems10050146).
- Zheng, B., Zhou, D.-W., Ye, H.-J., & Zhan, D.-C. (2023). Preserving locality in vision transformers for class incremental learning. *arXiv preprint arXiv:2304.06971*, . doi:[10.48550/arXiv.2304.06971](https://doi.org/10.48550/arXiv.2304.06971).
- Zhou, S., Zhang, S., & Linna, X. (2023). Research on analysis and application of quantitative investment strategies based on deep learning. *Advances in Computer Science and its Applications*, . doi:[10.25236/AJCIS.2023.061004](https://doi.org/10.25236/AJCIS.2023.061004).
- Zou, W., & Xia, Y. (2018). Back propagation bidirectional extreme learning machine for traffic flow time series prediction. *Neural Computing and Applications*, . doi:[10.1007/s00521-018-3578-y](https://doi.org/10.1007/s00521-018-3578-y).